THESIS FOR THE DEGREE OF DOCTOR OF PHILOSOPHY

Artificial and Intercellular Lipid Nanotubes

HAIJIANG ZHANG

Department of Chemical and Biological Engineering
CHALMERS UNIVERSITY OF TECHNOLOGY
Göteborg, Sweden 2013

Artificial and Intercellular Lipid Nanotubes

HAIJIANG ZHANG

ISBN: 978-91-7385-857-1

Doktorsavhandlingar vid Chalmers tekniska högskola

Ny serie Nr. 3539

ISSN: 0346-718X

Department of Chemical and Biological Engineering

Chalmers University of Technology

SE-412 96 Göteborg

Sweden

Telephone + 46 (0)31-772 1000

Back cover photo by Peter Sandin

Printed by Chalmers Reproservice

Göteborg, Sweden 2013

Artificial and Intercellular Nanotubes

HAIJIANG ZHANG

Department of Chemical and Biological Engineering

Chalmers University of Technology

Abstract

In this thesis work, we investigated the formation and shape dynamics of artificially created lipid nanotubes, and explored the on-demand generation of intercellular nanotubes. Methods and techniques to produce networks of phospholipid vesicles and lipid nanotubes, as well as networks of biological cells and lipid nanotubes, are described in this thesis. We also describe means to transport membrane material and network-internalized molecules and particles through the nanotubes. The capabilities, limitations and experimental requirements of these methods were analyzed. Starting from simple networks interconnecting two giant liposomes, free-floating floating lipid nanotubes were produced by electrofission. After releasing a lipid nanotube of several hundreds of micrometers in length from its suspension points, shape transformations through different stages were observed and characterized, and the influence of membrane-embedded molecules on these transformations were established.

A method was developed for on-demand generation of nanotubes between biological cells by means of micromanipulation and microinjection techniques originally developed for vesicle-nanotube networks. The new experimental model structures can greatly facilitate fundamental studies of cell-to-cell communication, the exchange of cell constituents and components, and the dynamics of biochemical reactions in native cell environments.

Lastly, we investigated the cells' capability to probe free space in its immediate vicinity. We designed a micropatterning strategy for selective cell immobilization and directed cell growth. A new microfabrication protocol for high-resolution pattern-generation of Teflon AF was developed for that purpose. The new surfaces enabled cell growth in specific orientations to each other, which allowed us to determine the distance-requirements for tunneling nanotube-like conduit formation.

The research results collected in this thesis represent a systematic approach towards on-demand generation and application of intercellular lipid nanotube connections, which is of importance for the understanding of, and eventually, full control over cellular communication networks.

Keywords: Nanotube Vesicles Network, Free-floating lipid nanotube, Artificial intercellular nanotube network, Microfabrication, Teflon AF.

List of Publications

This thesis is based on the work contained in the following articles:

I. **Generation of phospholipid vesicle-nanotube networks and transport of molecules therein**
Aldo Jesorka, Natalia Stepanyants, Haijiang Zhang, Bahanur Ortmen, Bodil Hakonen, Owe Orwar
Nature Protocols/VOL.6 NO.6/2011/791-805

II. **Spontaneous shape transformation of free-floating lipid membrane nanotubes**
Natalia Stepanyants, Haijiang Zhang, Tatsiana Lobovkina, Paul Dommersnes, Gavin D. M. Jeffries, Aldo Jesorka, Owe Orwar
Soft Matter, DOI: 10.1039/c3sm50429h

III. **Artificial nanotube connections and transport of molecular cargo between mammalian cells**
Haijiang Zhang, Shijun Xu, Gavin D. M. Jeffries, Owe Orwar, Aldo Jesorka
(Submitted to Nano Communication Networks)

IV. **Microgap closing by cellular processes-critical length-scales and membrane morphology**
Haijiang Zhang, Anna Kim, Shijun Xu, Ilja Czolkos, Gavin D. M. Jeffries, Owe Orwar, Aldo Jesorka
(Manuscript)

Contribution Report

Paper I: Contributed with experimental work, and participated in writing of the paper.

Paper II: Contributed to the original design of the experiments, and experimental work. Performed microscopy experiments and analyzed data.

Paper III: Contributed with entire experimental parts, performed experiments and analyzed data, and wrote the main body of the paper**.**

Paper IV: Contributed with entire experimental parts, performed experiments and analyzed data, and wrote the main body of the paper**.**

Contents

Chapter 1 Introduction

The cell membrane is a fundamental component of biological cells [1]. It consists of a self-assembled lipid bilayer of greatly varying composition [2], which surrounds the cytoplasm. Besides lipids [3], it features a multitude of different chemical species associated to it or embedded in it, mainly carbohydrates, and proteins [4]. The proteins are responsible for various structural and functional aspects of the cell [5-6]. Structural proteins provide shape and support, receptor proteins fulfill communication and signaling tasks with the external environment, transport proteins control the flow of molecules across the membrane, and glycoproteins are involved in tasks such as immune response, regulation and development, transport and structural response, and many others [7].

The cell membrane not only maintains and protects cell integrity, identity and shape, but also provides and supports vital biological functions. Cell adhesion, cell division, and selective permeability are some of the basic functions involving the plasma membrane [1]. Some complex processes, for example, the control of signaling pathways [8], might occur via regulation of cell size and shape. Intracellular signaling of cell volume regulation [9-11] involves, for example, membrane tension and membrane potential sensing. A variety of ion channels are activated by membrane stretching due to increased tension of the cell membrane [12].

Lipid molecules, as major fundamental components of cell membranes, are of special importance for this thesis. A briefly introduction can be found in Chapter 2. Because of their amphiphilic character, they will self-assemble in an aqueous environment into a double layer, or molecularly thin film, of a typical thickness of approximately 4-5 nm [13]. Lipid bilayers spontaneously reorganize to assume an energetically optimal geometric shape, such as a spherical vesicle [14-15], which is considered to be the most stable bilayer geometry [16]. Lipid vesicles are broadly used in many fields, such as drug delivery [17], DNA delivery [18-19], and in the cosmetic and food industries [20-22].

Lipid membranes are also known to form tubular structures, with a length up to several hundreds of micrometers, but only ~100 nm in diameter. Lipid nanotubes were first observed in connection with red blood cells [23], and between the Golgi apparatus and the endoplasmatic reticulum (ER) [24]. The cylindrical lipid structures with a

hollow (fluid-filled) interior are formed by lipid bilayer re-organization, or forced shape transformations [25-26].

In related experimental studies about two decades later, lipid bilayer vesicles were utilized as sources to generate nanotubes artificially, and construct lipid nanotube-vesicle networks (NVNs), which constitute excellent model systems for studying intercellular tubular membrane communication, and enzymatic reactions in confined spaces [27-28], as biosensors [27-29], for gene delivery [30], sol-to-gel transitions in polymers [31-32], and membrane-bimolecular interactions [33-34]. These networks were built and modified by applying micromanipulation and microinjection techniques [35]. The radius of these artificial, vesicle-interconnecting lipid bilayer nanotubes is approx. 50 to 100 nm, which was independently confirmed by several methods, the latest report used a mechanical approach [36]. A number of transport mechanisms inside the networks were also analyzed [30, 35, 37]. A detailed description of nanotube-vesicle networks, their properties, fabrication and a variety of means for materials transport is presented in **Paper I** in this thesis [35].

Lipid nanotubes are typically generated by applying a point force to a membrane, and they are suspended between membrane anchor points [35, 38]. If such a tube is released on one end, it retracts and merges with the membrane holding it on the other end, reducing its surface free energy in the process. An interesting, rather exotic shape transformation of a circular lipid nanotube has been reported in 2008 [39]. In a related study presented here in this thesis, the fate of free-floating lipid nanotubes, which was similarly released by an electro-cutting protocol, has been investigated. We observed a membrane folding mechanism of lipid bilayers at the end of individual free lipid nanotubes after being released (**Paper II)**.

In 2004, tunneling lipid nanotubes (TNT) were discovered as a new mode of intercellular communication in mammalian cells [40]. These tubular membrane channels could reach several cell diameters in length, and were 50 nm to 200 nm in diameter [40]. It is assumed that tubes help cells to mediate the transport of intercellular organelles, and cellular components, to aid in cell signaling [40-45] and to achieve long-range electric coupling of cells [46], Even nanotube-mediated routes to HIV transmission [47-48] were discovered.

It is a captivating idea to utilize the micromanipulation techniques developed to build NVNs in order to create nanotube connections between biological cells. Besides enabling new studies of membrane properties on the nanoscale, lipid membrane

nanotube vesicle networks were applied as models to study different transport modes and reaction kinetics in nanoscale environments. Similar fundamental studies could become possible in networks of cells, if intercellular (TNT-like) tube connections could be built at will. The exchange of cell constituents and components, the dynamics of biochemical reactions in native network environments, new experimental models for chemical cell-to-cell communication, and many other studies would become possible. In **Paper III**, we moved in this direction, and created the foundation for man-made network architectures involving biological cells. The experimental results demonstrate the validity and effectiveness of artificially created nanotube interconnections for chemical cell-to-cell communication.

In a related study, we focused on the fabrication of micropatterned surfaces suitable for observing the growth of tunneling membrane tube structures, and studied the ability of membrane protrusions to bridge obstacles of different length (**Paper IV**). Teflon AF microgaps, which represent artificial cytophobic barriers between approaching protrusions, prevent cellular growth and adhesion in the barrier region, and can thus be utilized to probe the cells´ ability to establish “through-space” connections with each other. The main idea was to see if a critical length scale exists, beyond which cells cannot probe free space, as well as to investigate the morphological features of the gap-spanning membrane. Importantly, we observed in these experiments the formation of nanotube junctions across microgaps up to 16 µm long.

Chapter 2 The lipid membrane

The cell membrane is an essential component of living cells. The cellular membrane provides various crucial functions, of which the most basic on is the barrier function. It allows selected materials to be transported into the cell, while preventing others to traverse the cellular membrane. Due to the selective permeability of the plasma membrane, cells and organelles are protected from the aqueous surrounding and can maintain their intracellular composition and homeostasis. Among the diverse functions of the cell membranes, the ability to perform shape and topology transformations is of special interest in the context of this thesis [7]. Many biological processes are influenced by shape transformations of membranes, such as cell division, endo- and exocytosis and transport of materials within and between cells. Some other examples involve tubulovesicular complexes for transportation of proteins between one endoplasmatic reticulum and Golgi complexes [24, 49].

The plasma membrane is a molecularly thin film (~5 nm). It consists of a lipid double layer: two sheets of lipid molecules facing each other, with proteins dissolved in the bilayer (Figure 2-1).

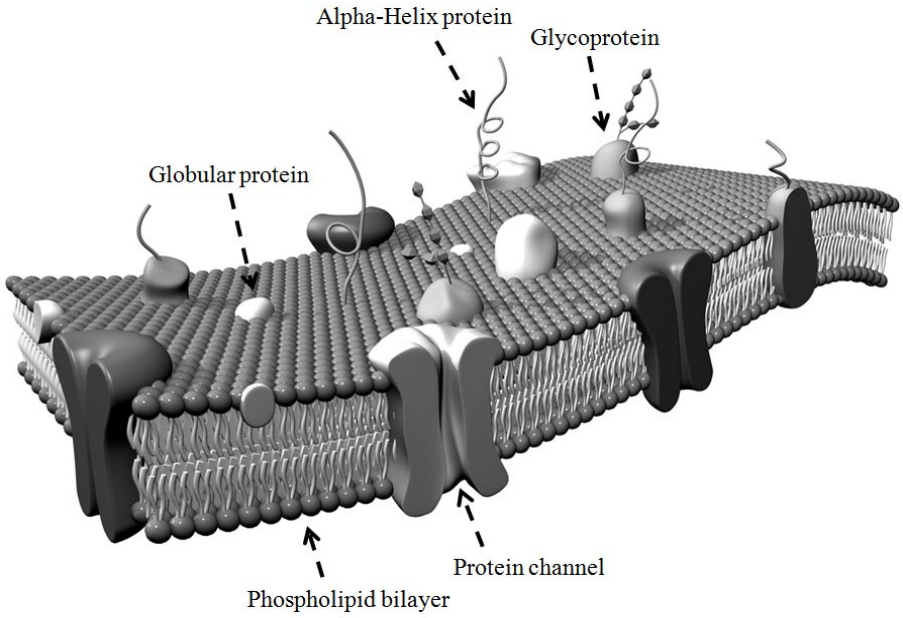

Figure 2-1 Schematic illustration of the structure of the cellular membrane. An iIndividual lipid molecule is represented by one head group and two tail groups. Various membrane proteins, such as ion channels and glycoproteins are embedded in the membrane sheets.

The membrane proteins constitute a considerable fraction of the cell membrane. In most animal cell membranes, proteins occupy almost 50% of the mass, the remainder being numerous types of different, albeit structurally related lipid molecules. In this chapter, the properties of lipid molecules, their self-assembly to lipid bilayer membranes and vesicles, and fundamentals of the mechanics of membrane shape deformations and membrane adhesion are introduced.

2.1 Lipids

Lipids can be broadly defined as fat-soluble organic molecules, which dissolve in organic solvents, such as alcohols and chloroform, but are insoluble in aqueous solutions. In biological cells there are numerous different lipid species such as sterols, fatty acids, gycerolipids, fat-soluble vitamins, sphingolipids, saccharolipids, polyketides, mono-, di- and triglycerides, and (glycero-) phospholipids. Phospholipids are the most abundant biological membrane lipids [50]. The structure of phospholipids contains two hydrophobic hydrocarbon tails (typical including 10 to 18 carbon atoms per chain) connected to a hydrophilic head group. A phosphate group links the hydrophilic head group to the rest of the molecule. Most abundantly found phospholipids in plasma membranes are phosphatidylcholine (PC), phosphatidylethanolamine (PE), phosphatidylglycerol (PG), and phosphatidylserine (PS). PC's hydrophilic head (choline) is linked via phosphate to glycerol, which is linked to the two hydrocarbon chains.

2.2 Lipid bilayer

When brought into an aqueous environment, phospholipids spontaneously aggregate and self-assemble as bilayers. This process is supported by the amphiphilic nature of the lipid molecule. Amphiphilicity (from Greek αμφις - amphis: both and φιλία - philia: love) arises if a molecule features both a hydrophilic (water-loving) and hydrophobic (water-fearing) moiety (Figure 2-3). In the next section, the result of self-aggregation- and the formation of the lipid bilayer – is discussed.

The structure of the bilayer resembles a sandwich. Its hydrophilic head groups face the aqueous environment, while the hydrophobic tails face each other in the interior of the bilayer Figure 2-2.

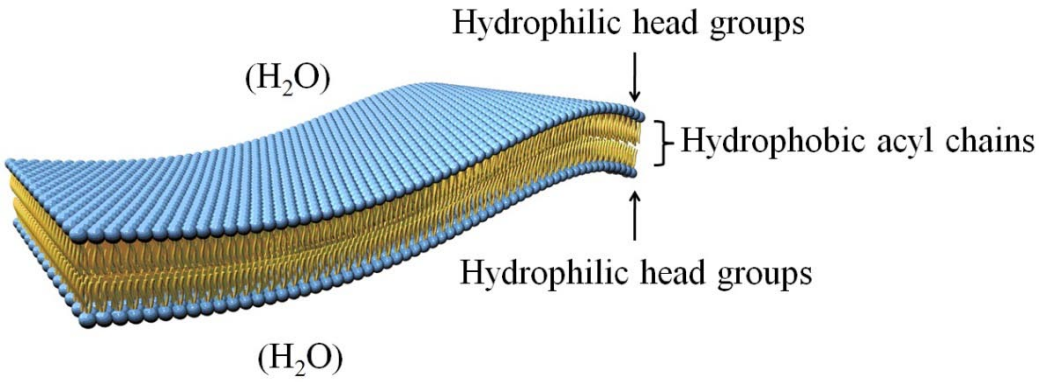

Figure 2-2 The phospholipids bilayer. The hydrophilic head groups are represented by blue colored spheres, and the hydrophobic acyl chains as pair of lines in yellow color. The hydrophobic tails face each other and form a shielded interior layer, much like the slices of a buttered sandwich.

The initially mentioned organization of the amphiphilic lipid molecules is energetically favored. In aqueous solution, water molecules continuously form hydrogen bonds with each other. When a lipid molecule is brought into this aqueous environment, hydrogen bonding is interrupted. In this situation, the hydrogen bonds re-organize to a higher order pocket structure to enclose the hydrophobic part (hydrophobic solvation). The amphiphilic molecule in this pocket is subject to two conflicting forces: the hydrophilic head being attracted to water and the hydrophobic tail seeks to avoid water, aggregating with other hydrophobic moieties. This thermodynamically driven interaction of molecules is called self-assembly (Figure 2-3). The free energy change (ΔG) occurring during self-assembly can be expressed as:

$$\Delta G = \Delta H - T\Delta S \qquad \text{Eq. 2.1}$$

$T\Delta S$ is the entropic contribution which encompasses the degree of order during the process of aggregation. ΔH is the change in enthalpy of aggregation. The hydrophobic pocket increases the degree of order among water molecules which causes the entropy to decrease. For the free energy to be minimized the degree of order in the system

should be reduced and the entropy should be increased. This is achieved by the self-assembly process, leading to the formation of a bilayer.

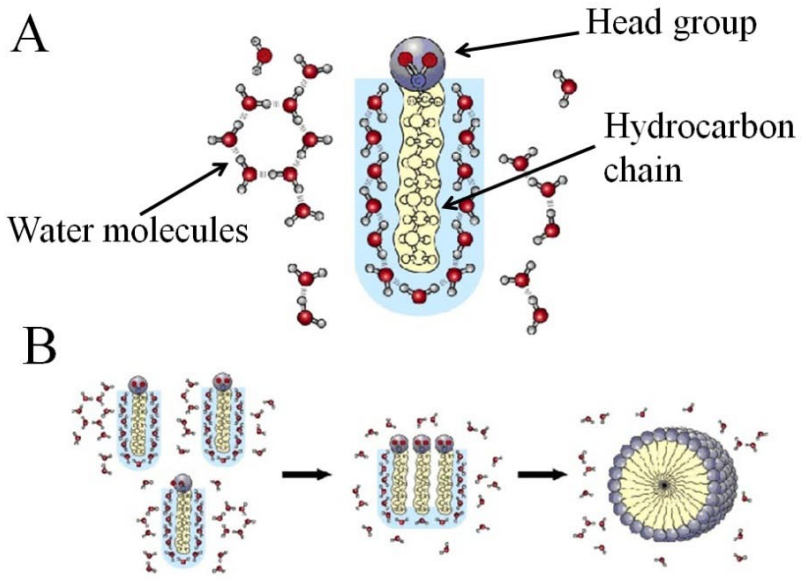

Figure 2-3 Self-assembly. (A) Hydrophobic pocket: A lipid molecule is surrounded by water molecules. Hydrogen bonding is interrupted. (B) As the concentration of lipid-like molecules increases, the hydrophobic parts start to aggregate, excluding the water molecules. This results eventually in self-assembly of lipid molecules to form a more organized structure, for example a spherical micelle, or a bilayer membrane.

I earlier introduced the cell plasma membrane barrier function. This important screening function is associated with the selective permeability of the lipid bilayer. The plasma membrane allows small hydrophobic molecules (such as O_2, CO_2, benzene *etc.*) and small uncharged polar molecules (such as H_2O, glycerol, ethanol *etc.*) to diffuse across, but is impermeable to larger uncharged polar molecules and ions, for example amino acids, glucose, H^+, Na^+ or K^+. This selective permeability originates from the hydrophobic interior of the bilayer, hindering the passage of the most hydrophilic molecules.

Different shapes of individual lipid molecules cause different types of aggregation shapes or geometries to be formed. The morphology of lipid molecules is described by the shape factor: $v_{ch}/a_0 l_{ch}$, where a_0 is the interface area occupied by the polar head group, v_{ch} and l_{ch} are the volume and length of the hydrophobic region,

respectively. The value of shape factors determines the final morphology of aggregation: micelles ($v_{ch}/a_0 l_{ch} < 1/3$), non-spherical (globular or cylindrical) micelles ($1/3 < v_{ch}/a_0 l_{ch} < 1/2$), bilayers or lamellar phases ($1/2 < v_{ch}/a_0 l_{ch} < 1$), and inverted micelles ($v_{ch}/a_0 l_{ch} > 1$) [51].

2.3 Lipid vesicles

The plasma membrane of a living cell is in fact a closed membrane compartment, encapsulating vital internal components and functions. Such closed compartments also exist *in vitro*, consisting solely of a spherical membrane composed of amphiphiles, featuring an encapsulated interior volume. They are referred to as vesicles, or in the case of lipid only compartments, liposomes. They have gained importance in biophysical research as versatile, easily produced, and easy-to-manipulate membrane model systems of the plasma membrane, and are of relevance in technological, medical and analytical applications [52]. In the following section, I will describe some fundamental properties of lipid bilayer vesicles.

A phosphobilayer membrane self-closes and entraps an aqueous solution to form a spherical structure: a liposome (or lipid vesicle). This spherical structure allows to entrap various molecules such as proteins, DNAs [53], RNAs [54], particles (*e.g.* nanoparticles) [55], or others. Vesicles have thus become important in medical research such as drug carriers [56-57] or in cosmetics to deliver skin products [20].

Lipid vesicles can be classified depending on the size and number of lipid bilayers (Figure 2-4). A unilamellar vesicle is composed of only one spherical lipid bilayer, a multilamellar vesicle has multiple bilayers, accordingly. Depending on their diameter, there are three major groups of lipid vesicles, referred to as small (10-50 nm), large (50-1000 nm) and giant vesicles ($> 1\ \mu m$) (Figure 2-4).

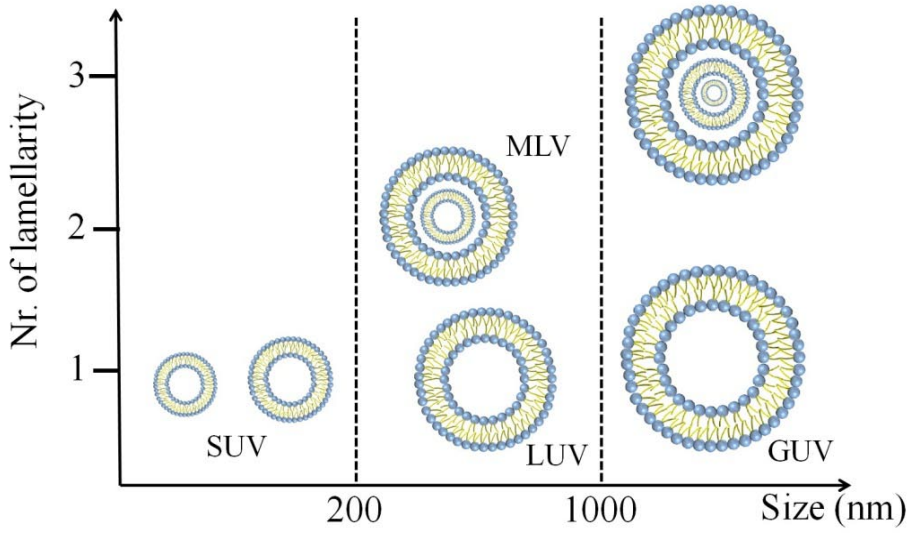

Figure 2-4 The classification of lipid vesicles in terms of their size and lamellarity. The unilamellar vesicles have diameters up to 50 nm and they consist of one single bilayer. Large vesicles can have one or multiple lamellae and have diameters starting from 50 nm up to 1µm. Giant vesicles, multi- or unilamellar, have dimensions of several tens or hundreds of micrometers.

In the experimental work for **Paper I**, electroporation and micromanipulation techniques were employed for the fabrication of lipid nanotube networks. Using these techniques, tubes were generated from unilamellar vesicles which were co-located with a multilamellar vesicle. The multilamellar vesicle acts like a reservoir of lipids, from which material is drawn to form the tube. Since unilamellar vesicles attached to a multilamellar reservoir are a peculiar, and rather rarely used form of vesicles, but indispensible for the generation of nanotubes from vesicle membranes, I will in the following briefly discuss the preparation of these vesicles.

There are various means available for preparing liposomes reproducibly. The choice of method depends mainly on the desired vesicle size, lamellarity, and of course, the intended application [52, 58-59]. In this work, a modified technique based on the dehydration & rehydration method has been used [60-61]. For this procedure, a thin lipid film is produced from an organic lipid solution, which is subsequently rehydrated for several hours, and sonicated to produce the vesicles. Aliquots of this suspension are dried on the intended substrate, and once again re-hydrated, forming twinned uni/multilamellar giant vesicles in good yield. In this swelling process, osmotic stress is very important for separation between lipid layers in the dried films [62].

2.4 Energy of lipid membranes

The experimental work for this thesis involves forced shape transformations and geometrical changes of lipid membranes, for instance the drawing of nanotubes, the "inflation" of vesicles, and other, non-trivial transformations (**Paper II**). It is therefore essential to be aware of the mechanical properties and features of lipid membranes, in particular with respect to their free energy. In this section, I will briefly describe the mechanics and energetics of lipid membranes.

Above the transition temperature (T_c), lipid membranes behave as a 2D liquid, and can be treated as a thin elastic shell. The currently prevailing theory applied to the mechanics of lipid membranes has been introduced by Helfrich in 1973 [63]. Two major types of membrane deformations covered by the theory are stretching and bending (Figure 2-5).

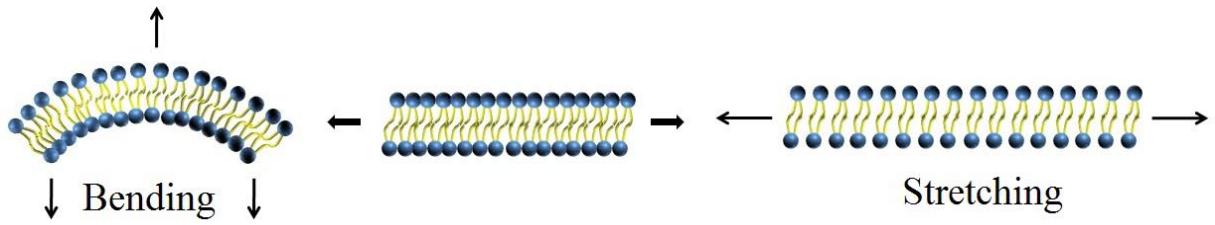

Figure 2-5 Fundamental deformations of a lipid bilayer membrane: Bending and stretching. In stretching, the distance between individual lipid molecules increases in both leaflets, therefore the membrane area increases. In bending, the distance between the molecules in the outer layer increases, while it decreases in the inner layer. Arrows show the directions in which the force is applied.

In this thesis, the shape deformations of lipid bilayer membranes arise from the effect of the applied mechanical forces. During these interactions, the total elastic free energy of a lipid bilayer membrane is increased. The free energy (E) can be written as [63-64]:

$$E = \frac{K_a}{2A_0}(A - A_0)^2 + \frac{K_c}{2}\int (c_1 + c_2 - c_0)^2 dA - \emptyset A^* \qquad \text{Eq. 2.2}$$

The fist term refers to stretching, where the membrane surface area is described by A_0 (before stretching) and A (after stretching) respectively. K_a is the stretching

modulus of the lipid membrane, which is typically in the order of ~240 mN/m [65]. During stretching, the number of lipid molecules in a given lipid bilayer membrane is constant. The stretching of the lipid bilayer membrane is looked upon as elastic dilation of the membrane, resulting in an increase of area per lipid molecule, while its hydrophobic core is increasingly exposed to water. Therefore the degree of stretching is limited: the maximum area expansion of lipid bilayer membranes is less than 5% [65-67]. Once this percentage increase in membrane area is exceeded, the lipid bilayer membrane ruptures, at a typical lysis tension of ~ 5-10 mN/m [66-67].

The second and third terms in equation 2.2 describe the bending of the lipid membrane. Two principal curvatures are described as c_1 and c_2, while c_0 is the spontaneous curvature. The spontaneous curvature accounts for a possible asymmetry of the lipid bilayer membrane, for example, for a different number of the molecules or a different lipid composition in the two lipid monolayer sheets [68]. In many cases for artificial vesicles, the spontaneous curvature c_0 is assumed to be zero, since both leaflets of the bilayer membrane are identical, as it is typically the case in our experimental system [69]. K_c is the bending modulus, which describes the membrane's resistance to bending. Typical values for K_c are in the range of $0.2{\sim}1 \cdot 10^{-19}\ J$ [70-71]. This corresponds to a few K_BT, where K_B is the Boltzmann constant and T is room temperature, which is a very small value compared to the energy required for membrane stretching, *i.e.*, a membrane can be easily bent, but resists stretching greatly. The last term in the equation represents the lipid bilayer membrane adhesion to the surface, as discussed separately below.

2.5 Adhesion forces and energy

For nanotube-vesicle networks to be generated and maintained, the lipid vesicles require immobilization on a rigid substrate. This requires surface interactions between the lipid bilayer and the substrate. When vesicles are suspended in an aqueous environment, they gradually sink down to the surface because of gravity. *Van der Waals*, electrostatic and hydration forces introduce a surface adhesion potential (typically at a distance in the range of several nanometers). The adhesion energy ($E_{adhesion}$) can be described as [63, 72]:

$$E_{adhesion} = \emptyset A^* \qquad \text{Eq. 2.3}$$

where $\emptyset$ is the effective contact potential, while A^* is the contact area of the adhering membrane. The adhesion energy depends on the cost in terms of bending energy, and affects the shape of the vesicle. During the process of adhesion, the shape of vesicle changes with the strength of adhesion as illustrated in Figure 2-6.

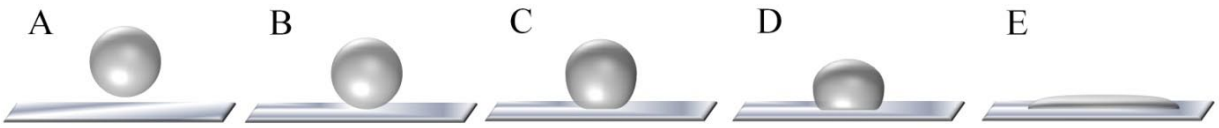

Figure 2-6 Adhesion of the vesicle on the surface. (A) A vesicle is approaching the surface due to gravitational force, so there is no contact potential. (B-D) Adhesion strength gradually increases. (E) The vesicle ruptures and spreads on the surface, after tension reaches a critical value (lysis tension).

The contact potential is zero in Figure 2-6 A. After the vesicle attaches on the surface [73], the contact potential can induce the deformation of the vesicle from spherical towards a truncated sphere as depicted in Figure 2-6 B-D. During this process, the stretching energy gradually replaces the bending energy to balance adhesion energy [72]. Once the contact potential becomes excessively large, tension-induced lysis occurs, the vesicle ruptures and spreads on the surface [74]. In this work, the high contact potential leading to rupture and supported film formation was eliminated by the employment of low-energy surfaces such as SU-8 [75], increasing the stability of the vesicle-nanotube networks significantly (**Paper I, II)**. On SU-8 surfaces, vesicles could neither spread nor rupture, maintaining a stable adhesion level long enough to build, modify and study the networks.

Chapter 3 Lipid nanotubes

3.1 Intercellular lipid nanotubes

In recent years, membrane nanotubes between biological cells have become subject to intensive research. Tunneling nanotubes sometimes referred to as "membrane nanotubes", "intercellular or epithelial bridges", or "cytoplasmic extensions" – are tubular membrane extensions that function as channels for intercellular transport and communication in many different cell types [76-77]. Intercellular communication is a central process in the development and maintenance of multicellular organisms. Several different short- and long-range communication routes between cells are known, including gap junctions [78], exosomes [79] and argosomes [80]. The tunneling nanotubes (TNTs) were discovered in 2004 by Rustom *et al*. as a new type structure for intercellular communication [40]. TNTs are thin membrane channels facilitating intercellular transport and communication between living cells. TNTs have been shown to emerge from the plasma membrane of cells in culture. Examples of TNTs between Human embryonic kidney (HEK 293) cells in culture from our own experimental observation are shown in Figure 3-1.

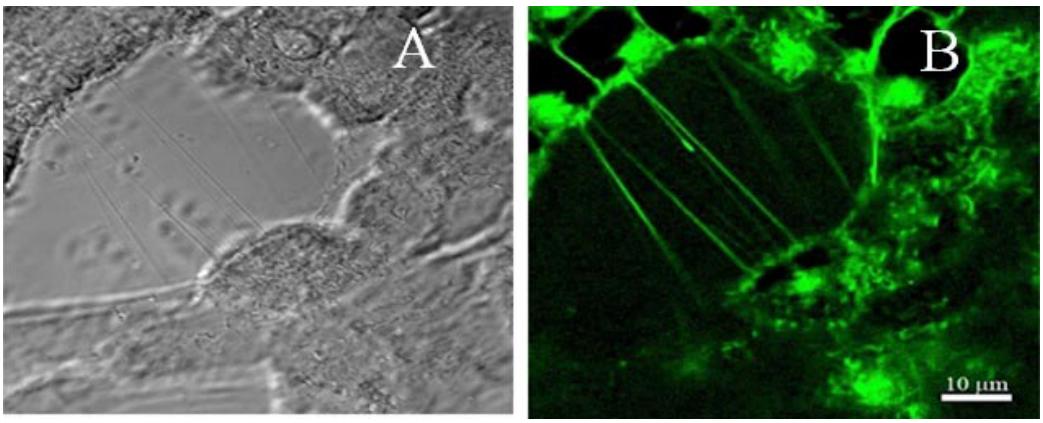

Figure 3-1 Inter-cellular tunneling nanotubes (TNTs). (A) Differential interference contrast and (B) fluorescence images of tunneling nanotube (TNTs), interconnecting human embryonic kidney (HEK 293) cells. The membranes are fluorescently labeled with the membrane dye FM 1-43.

TNTs *in vitro* mediate the transport of endosome-related organelles [40], cellular components [41], and signaling molecules [42]. They can also conduct medium-to-

long-range electrical signals [46, 81]. Bacterial communication has also been reported to be mediated by intercellular nanotubes [82], even nanotube-mediated routes to HIV transmission were suggested [47-48]. Besides inter-cellular communication, tunneling nanotubes can work as a connectors or transport channels between various intercellular organelles, for example, between the endoplasmic reticulum and the Golgi complex of mammalian cells [24, 83].

After the importance for cell-to-cell communication had been established, some research was conducted on developing TNTs formation strategies. Recently, the formation of TNTs during culturing was investigated employing microfabrication techniques [84]. A fraction of this thesis work is dedicated to artificial TNT-like tube connections in between cells. This work is in part based on fabrication techniques originally developed for the generation of lipid nanotubes from giant phospholipid vesicles [35].

3.2 Artificial lipid nanotubes

Lipid nanotubes or lipid tethers were first discovered during the exposure of surface-adhered red blood cells (RBCs) to hydrodynamic flows [23, 85]. In this particular study, the plasma membrane of the RBCs was initially anchored via adhesion points onto the substrate. As a result of shear stress caused by the flow, the cell lifted off from the substrate, but remained connected to it in some attachment points, such that the movement of the cell induced the elongation of the cell membrane as cylindrical protrusions. These protrusions were referred to as lipid tethers or nanotubes, and consisted of a hollow circular lipid bilayer membrane (Figure 3-2).

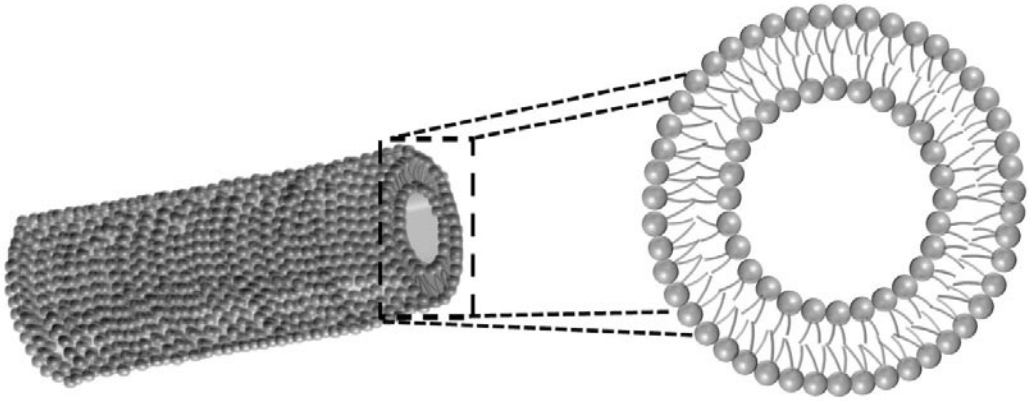

Figure 3-2 Schematic drawing of a lipid bilayer nanotube. The nanotube consists of a single bilayer wrapped up as a hollow cylinder (not drawn to scale). The enlarged section of the drawing shows the cross section of the lipid tube (inset). The diameter of the tube is typically between 50 and 200 nm.

Subsequently, a variety of experimental techniques were developed for the formation of nanotubes from lipid vesicles, including magnetic tweezers [86], optical tweezers [87], micromanipulation techniques [88] and motor proteins [34, 89]. In the experimental work conducted for this thesis, a combination of techniques including micromanipulation and micropipette electroporation were applied to form lipid nanotubes [38].

3.3 Fabrication of nanotubes and nanotube vesicle networks (NVNs)

Nanotube-vesicle networks (NVNs) are artificial constructs of micrometer and nanometer dimensions [90] that can, in this context, serve as versatile models for interlinked biochemical reactors [91]. NVNs can be fabricated from spherical bilayer membrane compartments by applying forced shape transition operations, which transform selected membrane regions into nanotubes and, subsequently, new liposomes. Electrical pulses are essential for manipulating the membrane of a liposome. A brief pulse will destabilize the membrane and form a pore. This electroporation method is of central importance in network fabrication, as stable pores allow facile introduction of microneedles with quite large orifices into bilayer containers (electroinjection).

In an electric field, the membrane can be regarded as a capacitor, in which charges are stored, resulting in a transmembrane potential [92-93]. If the field is of sufficient strength and duration, pore opening will occur, allowing the charges to dissipate. This instant process of formation of a membrane pore is illustrated in Figure 3-3. The radius of a pore decides its stability. The pore energy $E_{pore} = 2\pi a\gamma - \pi a^2\sigma$ describes the balance between the energy required to build the edge of a pore of radius α (first term) and line tension γ, and the energy gained due to the decrease in pore size under tension σ. If the radius is below a critical value $\alpha_c = \gamma/\sigma$, the edge energy dominates and the pore will close. γ is the line tension, while σ is lateral membrane tension. Otherwise, the dominating surface tension will lead to irreversible membrane breakdown. The extent of membrane permeabilization depends on pulse strength and duration, and the environmental conditions around the membrane, such as concentration, and temperature. If the pulse is too intense, the pores will expand beyond α_c and cause membrane rupture.

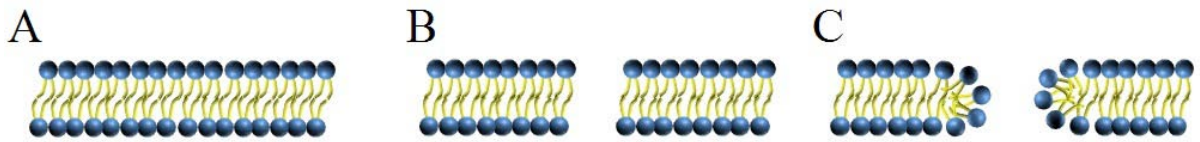

Figure 3-3 Pore formation in lipid bilayer membrane. Schematic shows the mechanism of pore formation in lipid bilayer membrane. (A) An intact lipid bilayer membrane. (B) A membrane pore is formed while applying an electric field of sufficient strength. (C) Lipid molecules are re-arranged at the pore edge in such way that hydrophilic head groups are exposed to water.

In a living cell, the transmembrane potential is constantly present across the plasma membrane. It can be used to drive the transport of ions and charged metabolites. For example, K^+ can be transported to the interior of the cells by potassium channels, while the value of the cell's resting potential is $-70mV$, which corresponds to a field strength of $200kV/cm$ over the 5 nm thickness of the membrane.

Another important function of electric fields in this work is in electrofusion and electrofission. Electrofusion involves a locally applied electric field, such that two lipid bilayers in close contact can be fused [94-95]. Electrofission describes the

opposite effect. A focused electric pulse is used to purposefully rupture the membrane. For example, in **Paper II**, we cut lipid nanotubes by electrofission from networks to observe their shape transformations.

In order to produce lipid nanotube vesicle networks, giant unilamellar vesicle-multilamellar vesicle complexes have to be prepared [90], as described above in section 2.3. The initial step in the formation of nanotube-vesicle networks is the immobilization of vesicles onto the substrate. This can be achieved by adding a suspension of vesicles to the observation chamber, typically a buffer droplet on a microscope cover slip, and allow it to precipitate. Subsequently, a borosilicate-glass micropipette (~0.25 μm outer-tip-diameter) filled with a buffer solution and a counter electrode, is placed close to the surface of a giant unilamellar vesicle. The micropipette tip can penetrate the membrane of the giant unilamellar vesicle by simultaneously applying a point force and an electric pulse (~ +20-40 mV, 8-10 ms pulse intensity/length) (Figure 3-4 A). The membrane then reseals around the micropipette tip. When the micropipette is pulled away, a lipid nanotube is formed between the micropipette tip and the vesicle (Figure 3-4 B). When the nanotube reaches the desired length, a positive injection pressure is applied and the buffer solution inside the micropipette is injected into the nanotube. As a result the nanotube forms a small vesicle at the tip of the micro-injection needle (Figure 3-4 C). The size of the formed vesicle can be controlled by the injection time. The newly formed vesicle can be positioned on the surface by gently pressing it to the surface (Figure 3-4 D). After the vesicle gets adhered onto the surface, the micropipette is pulled away while applying electrical pulses. The pipette gets detached (electrofission) and the remaining membrane pore reseals. By repeating this process several times, a complex network can be created.

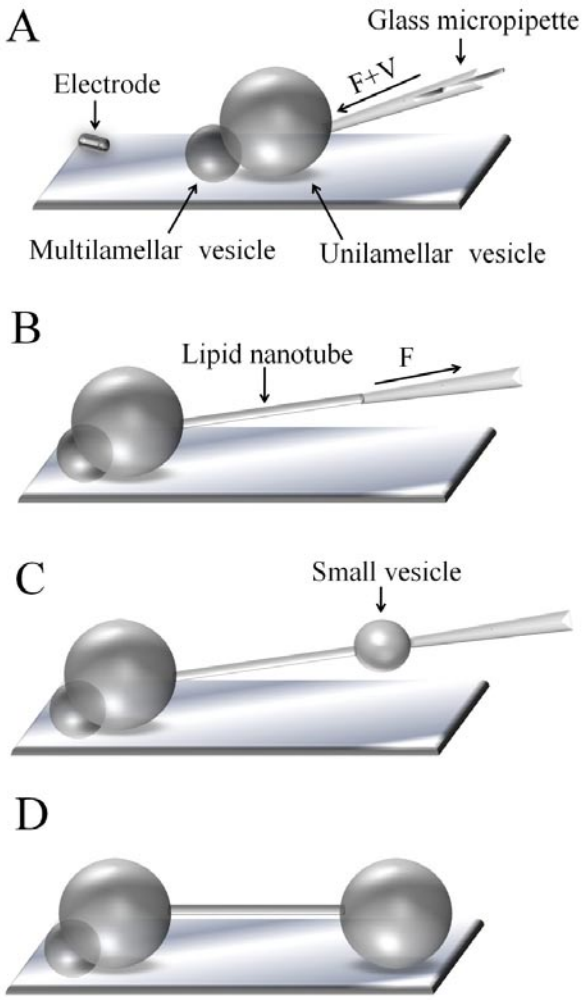

Figure 3-4 Formation of nanotube vesicle networks. (A) By applying a point force and an electric pulse to a surface-adhered vesicle, a micropipette penetrates the vesicle membrane. The pulse causes a pore in the membrane and the pore edge holds onto the pipette tip. (B) By slowly pulling the tip of the micropipette away from the vesicle, a lipid nanotube is formed (C) When buffer is injected into the nanotube by means of applying a positive pressure through the microinjection needle, a small vesicle is formed at its tip. (D) The new vesicle is adhered on the surface after reaching the desired size. Thereafter, the micropipette is detached from the new vesicle by electrofission.

Nanotubes generally have an unfavorably high surface free energy. This will cause them to minimize their length in order to decrease the surface free energy (spontaneous self-organization). In networks, this length minimization can cause a change in the structure of the network. For example, Y-junctions can be formed by this self-organization process when nanotubes merge in the network [96].

3.4 Energetics of lipid nanotubes

To be able to form a nanotube, a point force has to be applied to a vesicle. This force is approximately $10\ pN$, which is ~13% higher than the required force to extend an already formed lipid nanotube [97]. Because of the high bending energy in the nanotube, a fixed anchoring site is necessary, otherwise the tube instantly retracts. The free energy of a lipid nanotube is given by a combination of bending end stretching energies, and can be described as:

$$E_{nanotube} = \sigma A + \frac{\kappa}{2}\oint dA(\frac{1}{r})^2 = 2\pi r l\sigma + \frac{\kappa\pi l}{r} \qquad \text{Eq. 3.1}$$

where the first term represents the stretching energy, and the second term the bending energy of a lipid nanotube with principal curvature $\frac{1}{r}$. σ is the lateral membrane tension, r and l are the length and radius of the lipid nanotube, respectively. From the energy per unit length of the nanotube, the equilibrium radius of the tube can be obtained as $r_0 = \sqrt{k/2\sigma}$.

3.5 The mechanisms of transport in nanotube vesicle networks

There are three main transport modes between lipid vesicles through lipid nanotubes: diffusive motion of molecules or particles [98], tension-driven transport [37], and electrophoretic transport [13]. Protocols and requirements for all three transport modes are summarized in **Paper I**. Diffusive transport was investigated in nanotube-interconnected biological cells in **Paper IV**. This mode is an effective way for molecules to be transported via short distances or small volumes, which is typically the case with lipid nanotubes (Figure 3-5). It is the most common means of transport in NVNs, and is governed by the Brownian motion of molecules [91]. In order to traverse a nanotube, the size of the transported materials is required to be smaller than the tube diameter. The transport direction of molecules or particles is along the concentration gradient, from volumes of higher concentration towards the volumes of lower concentration. Directed diffusive transport (not Brownian motion) comes to a halt when the concentration reaches equilibrium.

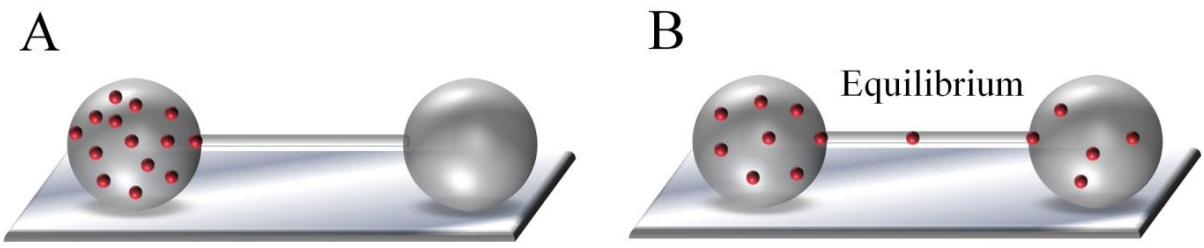

Figure 3-5 Diffusion transport. (A) Two vesicles are connected by one lipid nanotube, in a lipid nanotube-vesicle network. One of two vesicles is filled with particles, while the other of the two is empty. Particles start to diffuse along the concentration gradient from high to low concentration. (B) Diffusive motion stops once the concentration gradient disappears until concentration gradient disappearing.

Diffusive motion is determined by a concentration difference, which decays exponentially with $e^{-t/\tau_{relax}}$, where τ_{relax} is the relaxation time [98-99]. The relaxation time is defined as:

$$\tau_{relax} = \frac{V_1 V_2}{V_1 + V_2} \frac{l}{\pi r^2 D} \qquad \text{Eq. 3.2}$$

where l is the length of the lipid nanotube, while $V_1 and\ V_2$ are the volumes of the two vesicles. D is the diffusion coefficient for the molecule to be transported, and r is the radius of the nanotube. Based on this equation, it is apparent that the length of the lipid nanotube is an important parameter to determine the relaxation time. Generally, the diameter of a lipid nanotube is around 50-200 nm, while the radius of a vesicle is ~10 μm. In such nanoscale systems, relaxation times are on the order of hours, and not of days as in fluidic systems with micrometer channel diameters.

Besides the relaxation time, there are two other important time parameters governing the diffusive motion. One is the traffic time ($t_{traffic}$) which is used to describe the required time for a molecule or particle to travel from one to another vesicle, that includes the time needed for as molecule to find the entrance to the lipid nanotube. $t_{traffic}$ can be estimated as:

$$t_{traffic} = \frac{R_{vesicle}^3}{D r_{nanotube}} \qquad \text{Eq. 3.3}$$

where $r_{nanotube}$ is the radius of the lipid nanotube, while $R_{vesicle}$ is the radius of vesicle containing the molecules or particles. The traffic time is related to the mixing time. It is described as [100]:

$$t_{traffic} \sim \frac{R_{vesicle}}{r_{nanotube}} t_{mix} \qquad \text{Eq. 3.4}$$

where t_{mix} is denoted by the corresponding mixing times $t_{mix}^{vesicle}$ and $t_{mix}^{nanotube}$. The time which is required for a molecule to mix in the nanotube ($t_{mix}^{nanotube}$) and in the vesicle ($t_{mix}^{vesicle}$) are comparable to each other $t_{mix}^{vesicle} \sim t_{mix}^{nanotube}$.

$$t_{mix}^{vesicle} = \frac{R^2}{D} \;\; and \;\; t_{mix}^{nanotube} = \frac{l^2}{D} \qquad \text{Eq. 3.5}$$

The radius of vesicle is much smaller than the length of the lipid nanotube, hence, t_{mix} is much shorter then $t_{traffic}$. It means that one molecule or particle requires a longer time to find the lipid nanotube entrance than is required to travel through the whole vesicle volume.

3.6 Freely-floating lipid bilayer membrane nanotube

A freely floating nanotube, released from both anchoring sites, can be obtained by electrofission, *i.e.*, through application of a localized electric field, at both ends of a suspended tube. Experimental details are described in **Paper II**. Driven to lower their surface energy, these nanotubes undergo shape transformation. For example, short lipid nanotubes and tubular protrusions emanating from cell plasma membranes have been reported to evolve into vesicle-like structures [39, 101]. Despite these initial observations of nanotube membrane rearrangement, the transformation mechanism or the morphology of the final structures has thus far not been accomplished. In this thesis work, the fate of free-floating lipid membrane nanotubes was determined. First, a lipid nanotube was formed as described in section 3.3. Once the tube had formed, a second micropipette was used to apply an electrical pulse to the other end of the tube, simultaneous with the primary pipette (Figure 3-6 A). This causes the lipid nanotube to be released from both anchoring sites at once Figure 3-6 B.

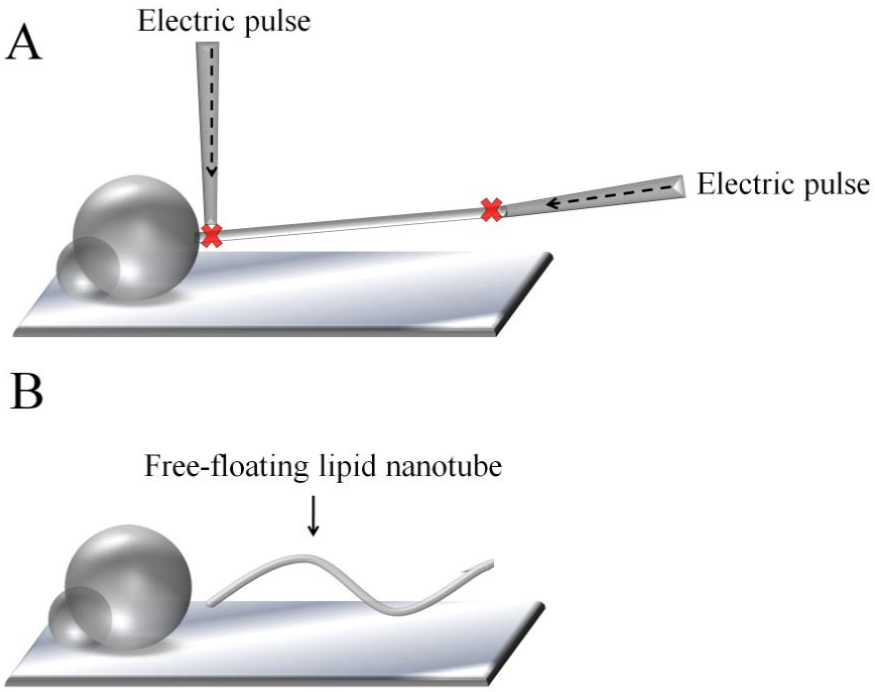

Figure 3-6 Fabrication of a free-floating lipid bilayer membrane nanotube. (A) After pulling a nanotube from a unilamellar vesicle, it was released by applying an electric pulse (red cross) from two micropipette tips simultaneously, producing a free-floating lipid nanotube (B).

After release, the shape of such a free-floating lipid nanotube is unstable, because of its high curvature energy, as compared to a spherical vesicle ($E = 8\pi\kappa \approx 250 k_B T$) [69, 97]. Therefore, the shape transformation from an initially tubular structure to a final stomatocyte-like structure occurs (Figure 3-7).

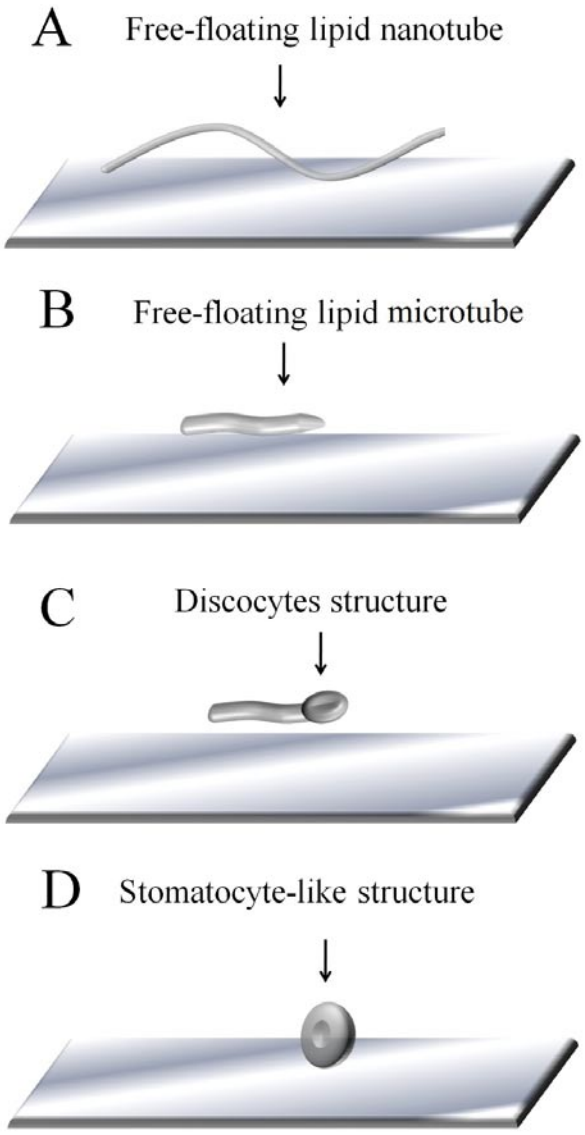

Figure 3-7 Shape transformation of a free-floating lipid nanotube into a stomatocyte-like structure. (A) Fee-floating nanotube in the solution. (B) Shape transformation to a microtube. (C) Discocyte structures appear on the tube, and consume lipid materials from tube. (D) Formation of stomatocyte-like structure as final shape without any significant volume change.

For such a transformation, the lipid transport between areas of the outer and the inner leaflet in the nanotube can be estimated from:

$$\Delta A = A_{+} - A_{-} = 2\pi dl \qquad \text{Eq. 3.6}$$

where d is half of the bilayer thickness. Lipid transport between leaflets is typically much faster in a nanotube than in vesicle [102], because of the high curvature. Our data implies an unconventional interleaflet lipid transfer rate (**Paper II**).

3.7 Intercellular nanotube networks

In 2011, Dubey and Ben-Yehuda reported that intercellular nanotubes could be formed between bacterial cells for exchange of cytoplasmic contents [82]. This previously uncharacterized type of bacterial communication was mediated by nanotubes, interconnecting several neighboring cells to form a network. Using *Bacillus subtilis* as a model, the transfer of cytoplasmic fluorescent molecules and of non-conjugated plasmids between adjacent cells was demonstrated. The authors also showed that molecular exchange enables bacteria to transiently acquire nonhereditary resistance against antibiotics. It is apparent that cellular networks with interconnecting nanotubes are an interesting model system to study transport phenomena, as well as specific aspects of cellular function. In the content of this thesis, micromanipulation and microinjection techniques were utilized to artificially create such intercellular tubular connections. The work flow of the technique is summarized in Figure 3-8 and further elaborated in **Paper III**. It is based upon the technique developed for liposome network generation (see section 3.3). Due to the sensitivity of the cells (HEK 293), the experimental conditions needed to be adjusted, in particular the electroporation parameters. An appropriate working environment adopted to perform cell studies is also necessary. Generally, physiological temperature and 5% of CO_2 in the ambient atmosphere are required to guarantee cell survival. The total time to fabricate the network and observe the transportation should not exceed 3 hours. The aim of these experiments was to establish that a) the technique is translatable to living cells, b) open nanotube connections are formed, and c) that the cells survive the electroporation, tube formation and electrofission procedure. It was established that stable intercellular networks can be fabricated, and that diffusive transport of ions and of small molecules can be achieved without compromising cell health.

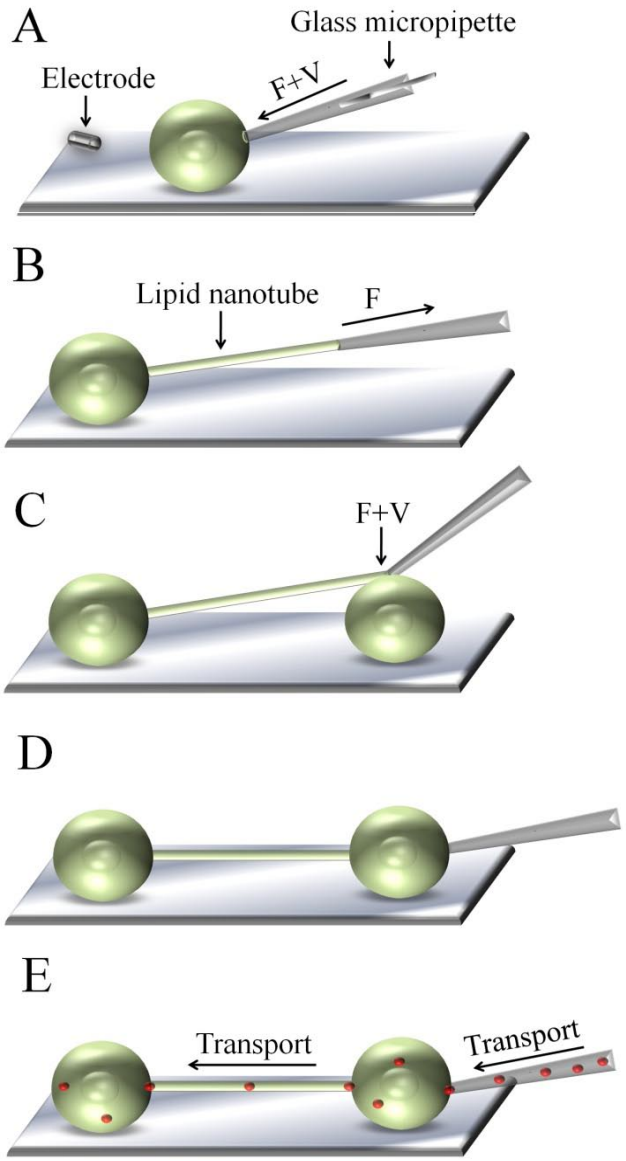

Figure 3-8 Fabrication of an artificial intercellular nanotube network, and transport experiments. (A) Glass micropipette penetrates the cell membrane following application of a combination of electric force and mechanical force. (B) A lipid nanotube is created by retracting the micropipette. (C-D) The formed nanotube is connected between two cells by applying similar forces as in A. (E) Particles diffuse from the micropipette via the mother to the daughter vesicle.

3.8 Surface-directed intercellular tubular membrane formation

Another interesting question with respect to cell-to-cell networks is related to the distance which cells can bridge in order to establish connections. We investigated adherent filopodia in HEK 293 cells and their capability to bridge Teflon AF micro gaps ranging from 2 to 16 µm. We intended to determine if there exists a critical length scale beyond which cells cannot probe free space, as well as to investigate the morphological features of the gap-bridging membrane. The cells' capabilities to probe free space are an important measure of how far cellular contacts can reach, and is probably cell type dependent. The basic experimental setup is illustrated in Figure 3-9. We adapted a general photolithography-based process, previously developed for the microfabrication of surface-supported Teflon AF structures, to fabricate cell culture substrates for investigating the ability of cells to overcome obstacles and form nanotubular interconnections. Teflon AF patterns primarily benefit from superior optical properties such as very low auto-fluorescence and a low refractive index, and can to assist directed cell growth along the structured surfaces. Cells develop in a guided fashion along the sides of the microstructures, selectively avoiding to grow over the patterned areas [103]. In our study we established that at a distance of 2-8 µm, the number of connections formed between cells via microgaps drops significantly. Experimental data and details are reported in **Paper IV**. The surface fabrication methods are discussed in detail in Chapter 4.

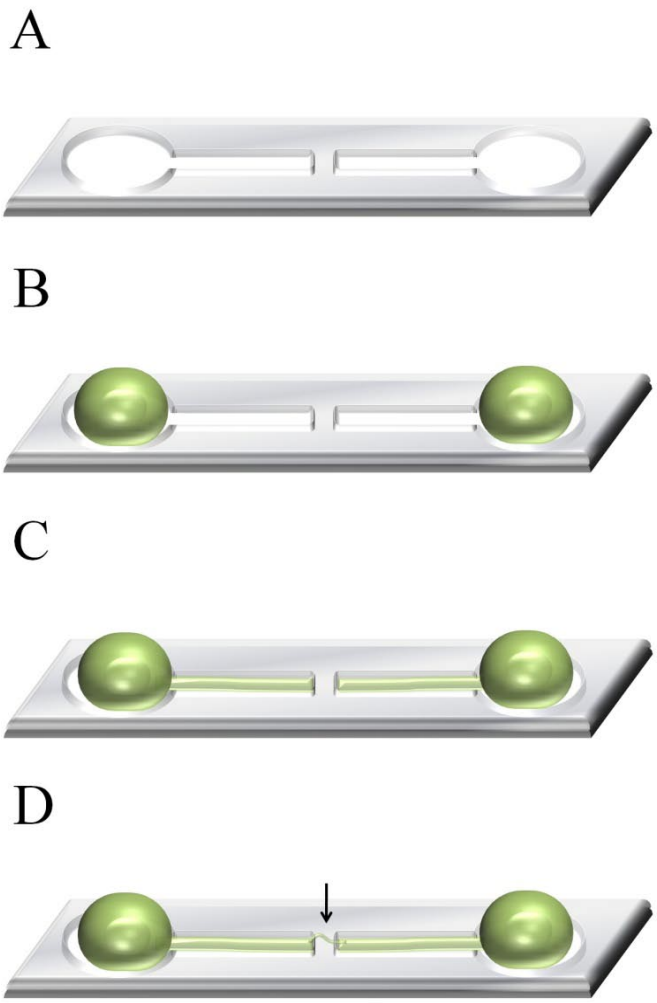

Figure 3-9 Growth and connection of tubular cell membranes on glass surface microchannels along with Teflon AF microstructure. (A) The cells are placed on micropatterned glass surfaces. The remainder of the cover slip is covered by Teflon AF. (B) After incubation, cells adhere to the circular patterns. (C) Tubular cell membrane grows along the glass microchannels. (D) After reaching the Teflon AF microgap, a cellular nanotube forms at the end of the tubular membrane (arrow), and attempts to cross over the Teflon AF microgap.

Chapter 4 Methods

4.1 Microfabrication

Microfabrication is the process of fabrication of miniature structures where the size scale is between 1mm and 100 nm. Below 100 nm, the term “nanofabrication” is commonly used, although the actual fabrication techniques involved can be the same, or closely related. Microfabrication uses integrated circuit manufacturing technology and complementary techniques, such as micromachining, lithography, etching and deposition. Microfabricated structures have found various life science applications, including tools for molecular biology, biochemistry and cell biology, further medical devices, and biosensors. Compared to conventional large scale devices, microfabricated devices and structures often feature enhanced functionality, and sometimes even novel capabilities [104]. For example, the whole field of microfluidics is entirely based on microfabrication processes. Microfludic channels are commonly fabricated using a combination of silicon wafer processing techniques, and specifically developed processes, such as polymer replica molding. The production costs of devices can be effectively decreased by microfabrication techniques, which is particularly apparent in the area of sensor fabrication [105]. A large number of examples for the use of small-scale devices in all areas of the bioscience research exist, for example in biomembrane, DNA, and protein research, as well as in bio-analytical chemistry [106-112].

In this thesis work, photolithography was used as the major technique for the fabrication of Teflon AF microstructures on glass cover slips. Details about the photolithography and our patterning process for Teflon AF are discussed in the following sections.

4.1.1 Photolithography

The basic concept of photolithography is to transfer a desired pattern onto a surface, using illumination of a photoactive coating material (resist) to define the pattern on the substrate. The light resource is typically ultraviolet (UV) light, which is in the right energy range to modify the chemical structure in the resist. Photolithography is in fundamental aspects related to photography. In both processes

light is used to transfer a pattern onto a light-sensitive film, either by using a pattern-defining mask, or directly without the mask. Photolithography involves the following basic steps:

i) Substrate cleaning, where contaminants are removed by wet chemical or plasma treatment.
ii) Surface preparation, where moisture is removed by the application of surface adhesion promoters or primers.
iii) Resist application, where the substrate is spin-coated with a resist solution to achieve a desired film thickness.
iv) Exposure, where the resist-coated substrate is exposed to intense UV light, which causes changes in the chemical structure of the resist, and enables development. In this step, the pattern is transferred to the photoresist, typically utilizing a photomask, which is an opaque plate with transparencies (dark field mask) or a transparent plate with opaque areas (bright or clear field mask) which allows light to shine through in a defined pattern.
v) Development, where either the exposed or unexposed areas of the light-treated resist film are selectively removed by treatment with a chemical developing solution.
vi) Pattern processing, where the substrate is altered in the areas that are not covered by the resist. This step physically transfers the pattern onto the substrate.
vii) Resist removal, or lift-off, where the unexposed resist is removed from the substrate by application of a solvent (resist stripper) or plasma treatment.

Figure 4-1 shows the main steps of the photolithographic process from resist application to development, depicting both the use of the bright field and dark field mask.

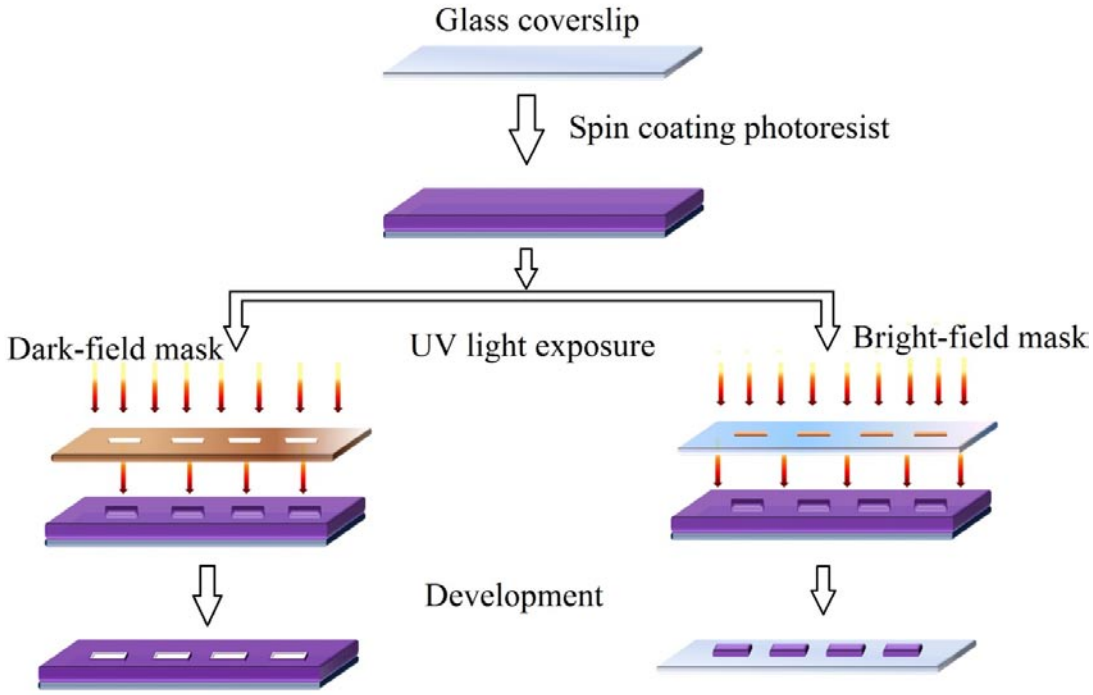

Figure 4-1 The flow of the photolithography process until development for a glass cover slip, which is the typical substrate used in this thesis work. The substrate cleaning step is omitted in the scheme.

Of considerable interest in the photolithographic process is the achievable resolution. The resolution of a lithographic process is formally defined by the modulation transfer function of the lithography exposure equipment, and the resist being utilized in it. In more practical terms, it refers to the ability to print minimum size images under conditions of typical process variation. The theoretical resolution in photolithography can be written for contact mode (no space between mask and substrate) as:

$$R = 1.5\sqrt{\lambda(\tfrac{z}{2})} \qquad \text{Eq. 4.1}$$

where λ is the wavelength of exposing radiation, and z is the thickness of the photoresist. The resolution of the practical lithographic process is influenced by process characteristic including: diffraction of light, lens aberrations, and the mechanical stability of the system (instrument), the properties of the resist material, and process details, such as soft-bake and post-bake conditions. Improvement of

optical resolution is continuously desired. Research is conducted on both the equipment and the photoresist chemistry aspects [113-116].

4.1.2 Patterning of Teflon AF

Teflon AF, an amorphous copolymers of polytetrafluoroethylene (PTFE) with 2,2-bis(triflouromethyl)-4,5-difluoro-1,3-dioxole is a very interesting modern material because of its characteristics: applicability to surfaces by spin-coating, strong hydrophobicity, high gas permeability [117]**,** and non-fluorescence. Teflon AF also features good biocompatibility. The low surface energy of micropatterned Teflon AF films could be exploited to achieve spatial control of cell adhesion. A number of biological cell studies were reported, where the cytophobic nature of Teflon AF was exploited for differential adhesion, further its tendency to guide cell growth [118-119]. However, Teflon AF is rather hard to combine with other materials due to its poor adhesion and insolubility, besides of micropatterning on special materials, such as silicon [120]. In our experimental work, Teflon microstructures were microfabricated on the glass surface of microscope cover slides. Fabrication details on the application of Teflon AF (1.2%(w/w) of solids) are presented in **Paper IV**. A brief work flow is presented in Figure 4-2.

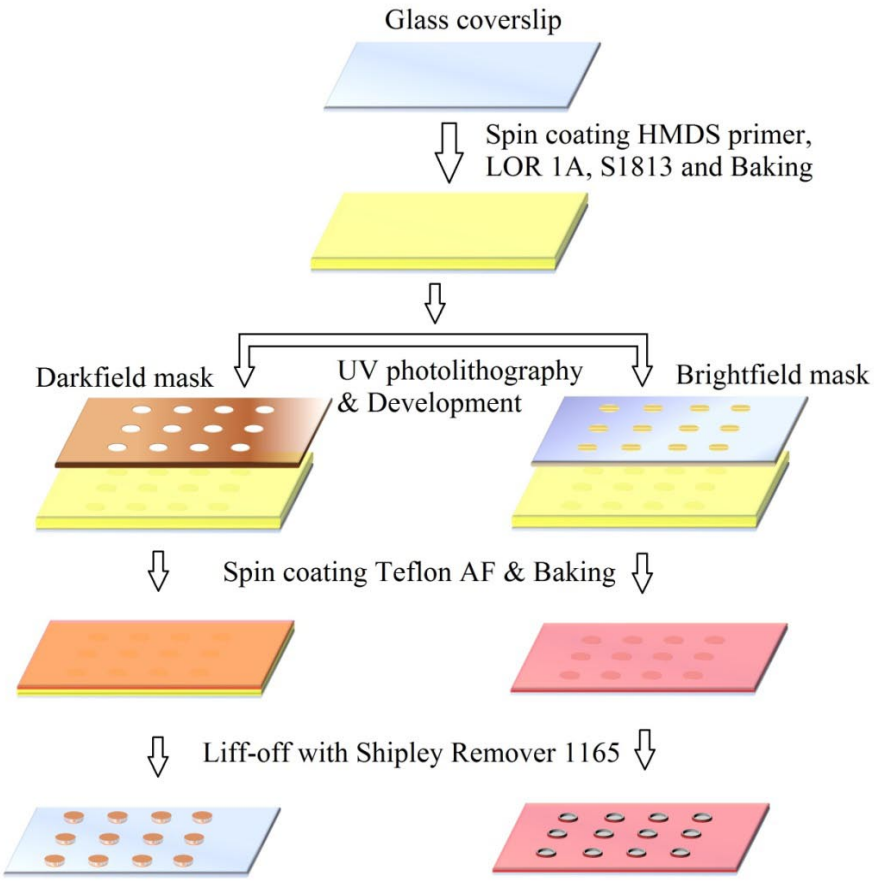

Figure 4-2 The microfabrication process for the deposition of Teflon AF microstructures onto glass cover slide surfaces. Teflon AF solution was spin-coated onto an exposed and developed S1813 resist layer, and the patterns are generated by lift-off of the photoresist film.

This photopatterning process is considerably simpler than previously reported processes [118], as it involves besides the exposure no other steps involving cleanroom instrumentation. However, the pattern adhesion to the glass cover slip is limiting the feature size to 1-2 µm. Surface treatment such as fluorosilanization [118] should bring improvement, but it would involve the deposition of a silicon oxide film as an additional step prior to photolithography.

4.2 Cell cultures

In this thesis work, cell culturing of mammalian cells was performed to provide specimen for the nanotube experiments described in **Paper III** and **IV**. Cell culturing is the process by which cells are grown *ex vivo* under defined conditions. Human Embryonic Kidney (HEK) 293 cells, Neuroblastom cell line NG 108 and Chinese Hamster Ovary (CHO) cells were the cell lines cultured and used in the experimental work. The basic steps which are required to prepare the cells for use in microscopy experiments are depicted in Figure 4-3.

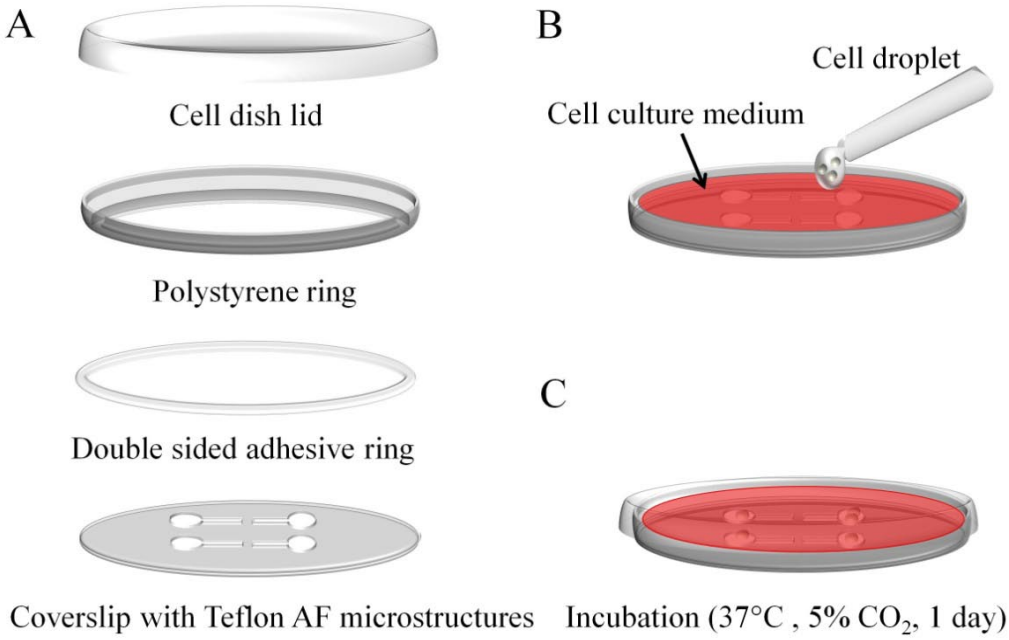

Figure 4-3 Culturing of cells for microscopy experiments. (A) A sterile glass plate (either patterned or unpatterned) is combined with a frame to assemble a culture dish, which is used directly under the microscope. (B) Cell culture medium and cell stock are combined in the dish. (C) Incubation under optimal growth condition 37 °C and 5% CO_2 for a desired time (~1 day).

WillCo glass bottom dishes, consisting of a plastic frame, glass cover slides and a double sided adhesive tape, were used to assemble culture dishes. In contrast to ordinary commercial culture dishes, his construction kit allows the use of pre-treated, or specially functionalized cover slides, such as the ones with microfabricated Teflon AF structures. After transfer of the cells into the assembled dishes, and incubation for

a desired time, microscopy experiments on the cells were performed (**Paper III** and **IV**).

4.3 Microscopy

The term “microscopy” summarizes instrumental techniques to view objects which are too small to be seen with the naked eye. A large variety of different techniques has been developed since the first microscope was built in ~1670. In the thesis work, optical microscopy was employed. Optical, or light microscopy, uses visible light, which is transmitted through the sample through a system of lenses, providing a magnified view of the sample. The image produced by the microscope can be viewed by the eye, or captured by various means, nowadays most commonly in digital format by electronic cameras. In optical microscopy, differences in intensity or color create image contrast, which makes individual features and details of the observed sample visible. Contrast can be defined as difference in intensity between a feature and its background relative to the overall background intensity. It is produced in microscopy by various means, for example by the absorption of light, by reflectance, color variations, or fluorescence. The ability to distinguish individual features in the image produced by the microscope is also related to the resolving power, also frequently termed resolution. The resolution depends on the numerical aperture (N.A.), which is a measure of the light collection capability of the objective.

$$N.A. = n \sin\theta \qquad \text{Eq. 4.2}$$

where n is the refractive index of the objective immersion medium, and θ is the maximum angle relative to the objective axis from which the objective can collect light. The resolution (r_λ) depends on N.A. and wavelength (λ).

$$r_\lambda = 0.61 \frac{\lambda}{N.A.} \qquad \text{Eq. 4.3}$$

In the thesis work, bright field microscopy with Differential Interference Contrast (DIC), Fluorescence Microscopy and Confocal Laser canning Microscopy were used.

4.3.1 Differential interference contrast microscopy

Differential Interference Contrast (DIC) is an illumination method to produce 3D bright field transmission images of sample without staining. It is a very useful technique to observe details of low contrast samples. The principle of the DIC imaging relies on light interference between two closely rays where one is slightly phase-retarded. The basic principle of this illumination technique is shown in Figure 4-4.

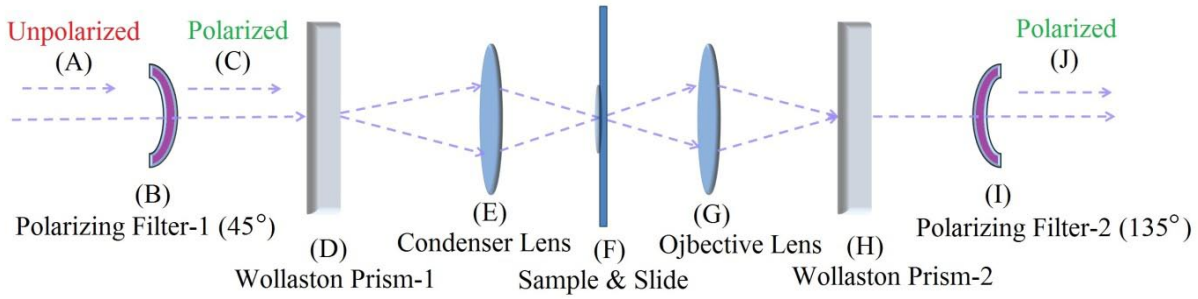

Figure 4-4 Light path through by Differential Interference Contrast (DIC) microscope. Unpolarized light (A) passes a (45º) polarizing filter (B), generating polarized light (C). It passes the first Wollaston prism (D) where it is split into two beams, which pass a condenser (E) and interact with the sample (F) From there the light continues through the objective Lens (G), pass the second Wollaston Prism (H), where the beams are recombined. A second polarizing Filter (135º) removes directly transmitted light from the polarized light (J).

As the polarized light is separated into two rays polarized at 90° to each other, the sampling and reference rays by the first Nomarski-modified Wollaston prism. Then, a condenser is used to focus the two rays onto the specimen. In which, two rays can not exactly focus on the same point, they are slightly apart by ~200 nm. Both rays experience different optical path lengths, if the areas they penetrate differ in refractive index or thickness. The rays travel through the objective lens, and are recombined by the second Wollaston prism into one polarized light ray. The recombination causes interference due to the path length difference, which is perceived as (enhanced) contrast in the generated image [121].

4.3.2 Fluorescence microscopy

Fluorescence microscopy is most commonly used in the biological sciences. It requires fluorescent specimen, which are either intrinsically fluorescent, or become fluorescent after staining, or labeling, by intrinsically fluorescent molecules. Such molecules can absorb light of a suitable wavelength (excitation) and subsequently emit light at a longer wavelength (emission). This process of light emission after excitation is referred to as fluorescence. The simplified Jablonski diagram in Figure 4-5 depicts the principle of fluorescence. After absorption of incident light, electrons are elevated from the ground state (S_0) into a singlet excited state (S_1) of higher energy. The excited electrons relax to a lowest energy level in the first singlet excited state (S_1) by vibrational relaxation on a timescale of 10^{-12} s. Then, the excited electrons return to the ground state (S_0), emitting a photon (fluorescence) within 10^{-7} to 10^{-9} s. In fluorescence microscopy, this light emission is responsible for the, typically, strong contrast. The emitted light can be collected and processed to form an image. The advantage of this method is the possibility to observe details of samples which show no contrast in ordinary light microscopy.

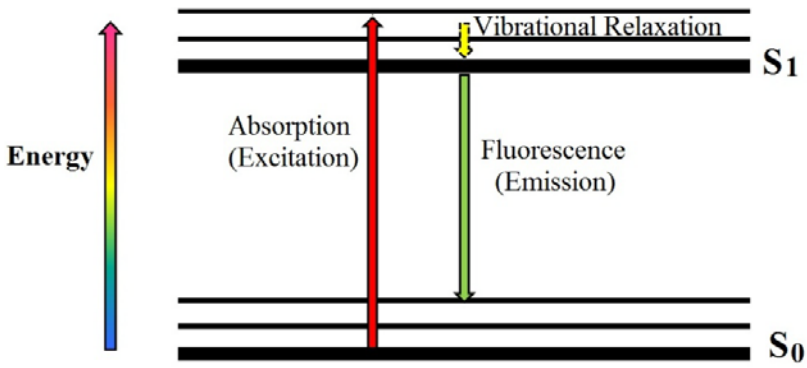

Figure 4-5 Simplified Jablonski diagram, depicting the fluorescence process.

High excitation intensities can be achieved by means of laser illumination (laser induced fluorescence, LIF). A variety of different wavelengths are today available for fluorescence microscopy, such as 488 nm (Ar^+) and 633 nm (He-Ne).

4.3.3 Confocal laser scanning microscopy

Confocal laser scanning microscopy (CLSM) is a modern fluorescence based microscopy technique, which provides exceptionally high optical resolution and contrast. Confocal microscopy utilizes point illumination and a spatial pinhole in front of the detector to eliminate out-of-focus light in objects that are thicker than the focal plane. The principle is illustrated in Figure 4-6.

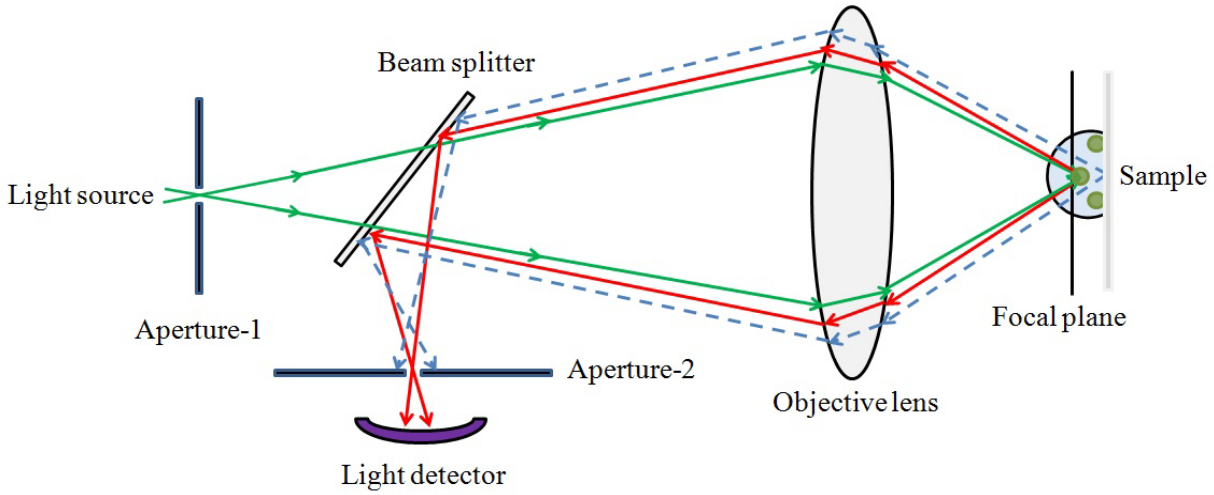

Figure 4-6 Principle of confocal microscopy. The light from the focal plane passes the pinhole and reaches the detector, while out-of-focus light is rejected at the pinhole.

In a confocal laser scanning microscope, a laser beam serves as light source. The technique use typically 2 or 3 mirrors to deflect the beam, scanning linearly along the x and the y axis, in order to move the laser beam across the sample. A fixed emission pinhole and detector are used, and the image is constructed point by point, according to the mirror movements. Thus, the sampling density is programmable and very high resolutions can be achieved. The confocal laser scanning microscopy was the most widely used method used in this thesis work.

Chapter 5 Summary of papers

Paper I.

Generation of phospholipid vesicle-nanotube networks and transport of molecules therein

In **Paper I,** the fabrication procedures for soft-matter tube & container networks, consisting of lipid nanoconduits and surface-immobilized vesicles, was described in detail, including lipid and surface preparation, micromanipulation and microinjection techniques. The micromanipulation techniques comprised membrane electroporation and microinjection, which were applied to effect shape transformations of the membrane in order to create tube-interconnected compartments. Passive and active transport of molecules and membrane material within the fabricated networks were also described, including diffusive, tension driven [122] and electric field-driven [30] transport. The vesicle-nanotube networks are suitable model systems for chemical reactions in confined spaces, dynamics of bilayer membranes and nanotubes, and starting points for various soft-matter nanodevices.

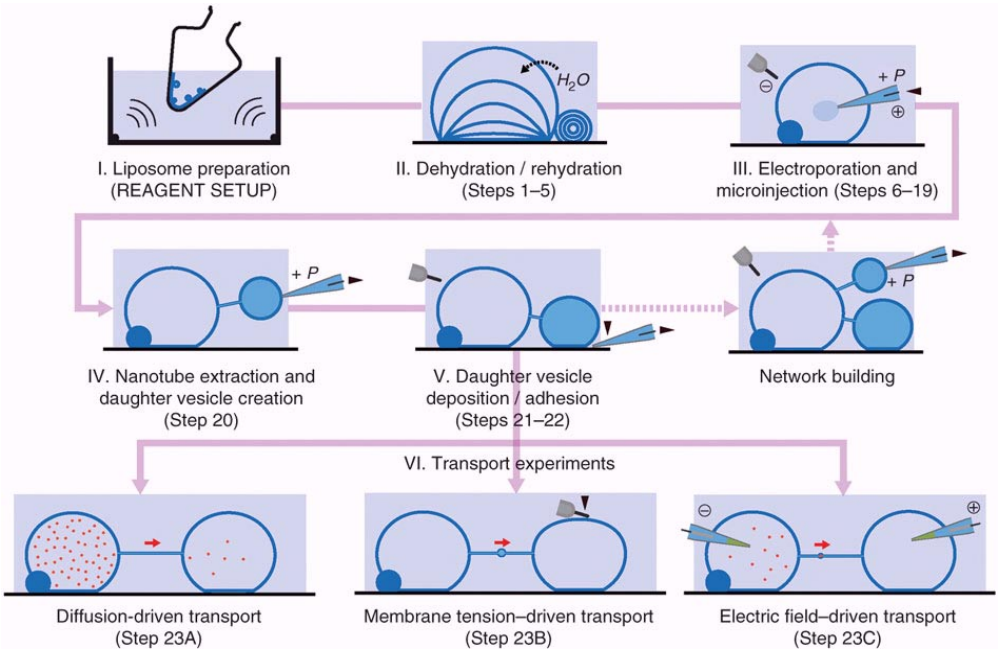

Figure 5-1 The soft-matter fabrication process for the generation of nanotubes-vesicle networks (I-V), and three individual modes of transport of small molecules and membrane material within the networks (VI).

Paper II.

Spontaneous shape transformation of free-floating lipid membrane nanotubes

The dynamics of free floating lipid nanotubes was reported in **Paper II**. A nanotube was pulled from a surface-adhered giant unilamellar vesicle in a buffer droplet, using a glass microneedle, and separated from both the needle and the vesicles by means of an electric pulse. After the release, the lipid nanotube, measuring several hundreds of micrometers in length, floated freely in the aqueous buffer droplet. Shape transformations through different stages were observed and characterized and the influence of membrane-embedded molecules on these transformations were established. To minimize the surface free energy, which is high in the free nanotube compared to a vesicle of the same surface area, the tube undergoes shape transformations, which proceed through several stages. Stomatocyte-like structures were determined as the final shapes. This stage was reached without any significant volume change, but under high curvature energy consumption during the transformation.

In the experimental work, membrane dyes (FM1-43 and Texas Red DHPE) were used to monitor the shape transformation dynamics, and quantitative fluorescence intensity analysis was employed to study membrane translocation inside the structures. Transformation rates were estimated. Nanotubes labelled with a water-soluble styryl dye, FM1-43, transformed approximately five fold faster than nanotubes labelled with the phospholipid conjugated dye Texas Red DHPE.

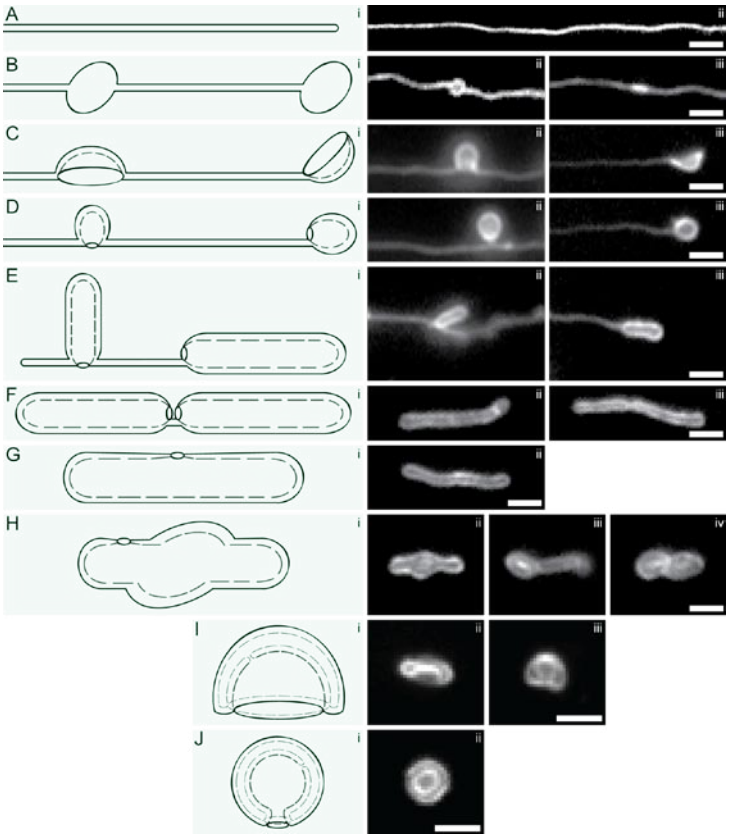

Figure 5-2 Folding model for shape transformation supported by snapshots of corresponding structures from recordings of the SPE-FM nanotube transformation. (A) A free-floating nanotube is formed. (B) Disc-like structures appear on the tube. (C-D) The disc-like structures begin to curve and develop into stomatocytes connected to a nanotube. (E-G) A double walled tube is formed after the entire nanotube being consumed. (H-J) Disc-like thickening appears, and bends to a stomatocyte. The scale bar corresponds to 10 μm in (A), and 5 μm in (B-J).

Paper III.

Artificial nanotube connections and transport of molecular cargo between mammalian cells

In **Paper III**, open nanotube connections are generated between a glass microneedle and a human embryonic kidney (HEK293) cell, and in between two cells. The micromanipulation techniques are adapted from **Paper I**. After construction of the needle/cell-to-cell connection, intercellular transport of molecular cargo was studied. In the experiments, calcium ions and pre-fluorescent enzyme substrate are transported to the connected cell by diffusion through the tube. In each of the experiments, the cell health status after generation of the nanotube was evaluated by means of superfusion of the cells with the diazo dye Trypan blue. Cell survival after nanotube formation was confirmed. This cell model can greatly facilitate fundamental studies of cell-to-cell communication, the exchange of cell constituents and components, and the dynamics of biochemical reactions in native network environments.

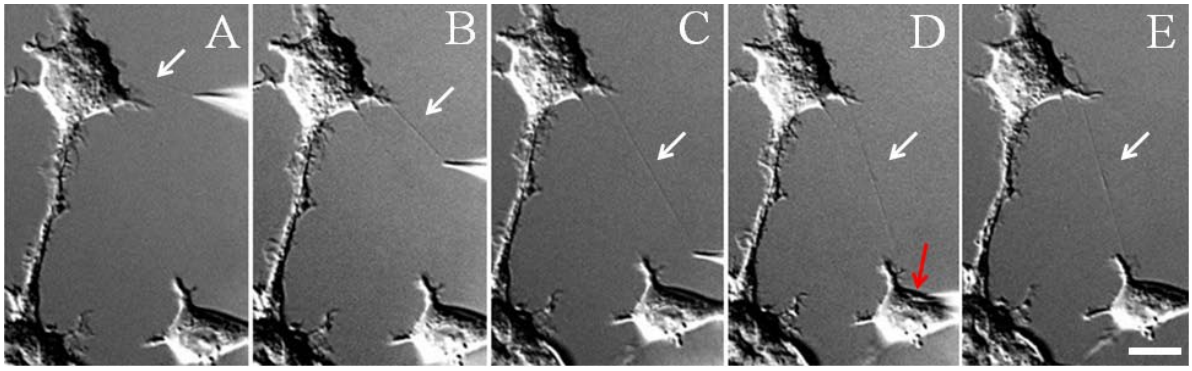

Figure 5-3 DIC images depicting the generation of an intercellular nanotube (white arrow) between two individual human embryonic kidney (HEK 293) cells. Scale bar: 10 µm. (A) A glass microneedle was used to penetrate the upper cell, and to draw a nanotube from it, using the micropipette procedure described in the text. (B-C) The needle is being translated towards the target cell, elongating the tip-attached nanotube. (D) By bringing the needle tip (red arrow) in contact with the cell and applying an electric pulse, the tube connects permanently to the cell membrane. (E) The glass micropipette tip has been retracted and disconnected from the cell, leaving behind an intercellular tube.

Paper IV.

Microgap closing by cellular processes-critical length-scales and membrane morphology

Paper IV reports a study on the capability of adherent filopodia of human embryonic kidney (HEK 293) cells to bridge Teflon AF microgaps. The purpose of the study was to determine if there exists a critical length scale beyond which cells cannot probe free space, as well as to investigate the morphological features of the gap-spanning membrane, *i.e.,* to investigate if nanotubes can be formed on microgaps in a controlled way. To achieve this goal, the lithography method is applied to micro-patterned substrates fabricated from glass and amorphous Teflon AF in the fashion described in **Paper III**. We grew HEK 293 filopodia on 2 μm wide glass microchannels intersected by Teflon AF microgaps of different lengths: 2, 4, 8, and 16 μm, respectively. After 1 day incubation, we observed that cell protrusions were able to span gap sizes of 2 and 4 μm in nearly all experiments, but larger gaps less frequently. Cell extensions crossing microgaps generally appeared as nanotubes in approx. 30% of all observed cases. By means of a microfluidic superfusion device, which was utilized to chemically porate one cell, and deliver a fluorescent compound to it, and the transport capabilities of cell-to-cell connections established in this way were probed. Figure 5-4

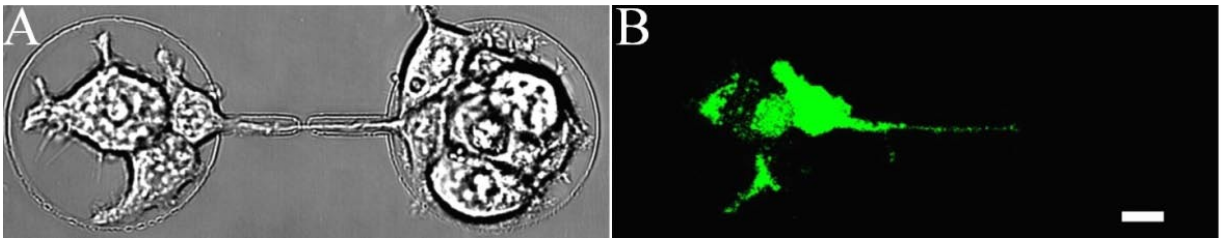

Figure 5-4 An example of chemical transport between two cells through a tubular interconnection, following directed growth of the cell-to-cell connection on glass microchannels, which are separated by a Teflon AF microgap. (A) Brightfield DIC image of a tubular interconnection across a 2 μm gap between two cells. (B) Hindered transport in the interconnection, which features a junction between the connected cells, visualized by fluorescein internalized in one of the cells. Scale bar: 10 μm.

Chapter 6 Conclusion and Outlook

In this Ph.D. work, we investigated the formation and dynamics of artificially created lipid nanotubes, and explored the on-demand generation of intercellular nanotubes. Methods and techniques to produce networks of phospholipid vesicles and lipid nanotubes, as well as networks of biological cells and lipid nanotubes, are described in this thesis. It also covers means to transport membrane material and internalized molecules and particles through the nanotubes, both in biomimetic networks, and between biological cells. The capabilities, limitations and experimental requirements of the techniques used in this work are described in detail in **Paper I**. Thereafter, the dynamics of individually generated nanotubes was investigated. Starting from simple networks interconnecting two giant liposomes, free-floating lipid nanotubes were produced, and the fate of the liberated nanotubes was determined. After releasing a lipid nanotube of several hundreds of micrometers in length from its suspension points, which was achieved by electrofission on both ends of the tube, shape transformations through different stages could be observed and characterized, and the influence of membrane-embedded molecules on these transformations were established (**Paper II**).

Paper III demonstrates the on-demand generation of nanotubes between biological cells by means of micromanipulation and microinjection techniques originally developed for vesicle-nanotube networks. These new model structures have the potential to greatly facilitate fundamental studies of cell-to-cell communication, the exchange of cell constituents and components, and the dynamics of biochemical reactions in native cell environments. It is the first report on cell-to cell connectivity established artificially. In **Paper IV** we focused on the cells' capability to probe free space in its immediate vicinity. We designed a micropatterning strategy for selective cell immobilization and directed cell growth. A new microfabrication protocol for high-resolution pattern-generation of Teflon AF was developed for that purpose. The new surfaces enabled growing cells in specific orientations to each other, which allowed us to determine the distance-requirements for tunneling nanotube (TNT)-like conduit formation. This work improves the performance of previous cell-nanotube platforms [84], and opens new possibilities.

The research results assembled in this thesis represent a systematic approach towards on-demand generation and application of intercellular lipid nanotube connections, which is of importance for the understanding, and perhaps eventually, for

the full control over cellular communication networks. In future work, more sophisticated cell-to-cell communication methods have to be developed, including communication by means of electrical signals. It is the cytophobic Teflon AF material which has proven to be of particular utility for directed growth and tubular interconnection formation. The fabrication strategies presented in this thesis provide a solid foundation for current and upcoming experimental studies.

Acknowledgements

I wish to express my gratitude and special thanks to the following people:

To my supervisor Owe Orwar, Thank you so much for giving me such a great opportunity to explore the fantastic membrane tube world. Thank you for believing in me!

To my co-supervisor Aldo Jesorka, Thank you very much for your good suggestions and useful discussions for my research project. Thank you so much for your advice, encouragement, help and support!

To Gavin D.M. Jefferies, Thanks a lot for your invaluable and positive discussion on my project. I got a lot of inspiration from you!

To Irep Gözen and Shijun Xu, Thank you so much! I appreciate your help and encouragement very much!

To the people in Orwar Research Group, you are so great!

To one special and the most important person in my life (my Mom):

Thank you Mom! Thank you for your love, endless support and encouragement! I wish that you are happy and health forever!! I love you, my great and self-confident Mom!!

To my pretty wife - Ti Chen! Thank you for your trust, support, and love! I love you! Jag älskar dig!

To my all friends and my family in Sweden and China! Thanks a lot for believing in me!

References

1. Alberts B., *et al.*, *Molecular Biology of the Cell. 4th edition*. 2002, New York: Garland Science.
2. Gennis R.B., *Biomembranes: molecular structure and function*. 1989, New York: Springer.verlag.
3. Phillips R., *et al*., *Emerging roles for lipids in shaping membrane-protein function.* Nature, 2009. **459**(7245): p. 379-85.
4. Gil T., *et al*., *Theoretical analysis of protein organization in lipid membranes.* Biochim. Biophys. Acta., 1998. **1376**(3): p. 245-66.
5. Andersen O. S. and Koeppe R. E., *Bilayer thickness and membrane protein function: an energetic perspective.* Annu. Rev. Biophys. Biomol. Struct., 2007. **36**: p. 107-30.
6. Garcia-Saez A. J. and Schwille P., *Single molecule techniques for the study of membrane proteins.* Appl. Microbiol. Biotechnol., 2007. **76**(2): p. 257-66.
7. Alberts B., *et al*., *Essential cell biology (second edition)*. 2003: Garland science / Taylor & Francis Group.
8. Meyers J., Craig J., and Odde D. J., *Potential for control of signaling pathways via cell size and shape.* Curr. Biol., 2006. **16**(17): p. 1685-93.
9. Haussinger D., Lang F., and Gerok W., *Regulation of cell function by the cellular hydration state.* Am. J. Physiol., 1994. **267**(3 Pt 1): p. E343-55.
10. Volkl H., *et al*., *Alkalinization of acidic cellular compartments following cell swelling.* FEBS Lett., 1994. **338**(1): p. 27-30.
11. Lang F., *et al*., *Functional significance of cell volume regulatory mechanisms.* Physiol. Rev., 1998. **78**(1): p. 247-306.
12. Yin J. and Kuebler W. M., *Mechanotransduction by TRP Channels: General Concepts and Specific Role in the Vasculature.* Cell Biochem. Biophys., 2010. **56**(1): p. 1-18.
13. Hurtig J., *et al*., *Electrophoretic transport in surfactant nanotube networks wired on microfabricated substrates.* Anal. Chem., 2006. **78**(15): p. 5281-8.
14. Edwards D. A., *et al*., *Spontaneous vesicle formation at lipid bilayer membranes.* Biophys. J., 1996. **71**(3): p. 1208-1214.
15. Israelachvili J. N., Mitchell D. J., and Ninham B. W., *Theory of self-assembly of lipid bilayers and vesicles.* Biochim. Biophys. Acta., 1977. **470**(2): p. 185-201.
16. Evans E. and Metcalfe M., *Free energy potential for aggregation of giant, neutral lipid bilayer vesicles by Van der Waals attraction.* Biophys. J., 1984. **46**(3): p. 423-6.
17. Cevc G., *Lipid vesicles and other colloids as drug carriers on the skin.* Adv.Drug.Deliver.Rev. , 2004. **56**(5): p. 675-711.
18. Babiuk S., *et al.*, *Topical delivery of plasmid DNA using biphasic lipid vesicles (Biphasix).* J.Pharm.Pharmacol., 2002. **54**(12): p. 1609-1614.
19. Guo X. and Szoka F. C. Jr., *Chemical approaches to triggerable lipid vesicles for drug and gene delivery.* Acc. Chem. Res., 2003. **36**(5): p. 335-41.
20. Lasic D. D., *Liposomes : from physics to applications*. 1993, Amsterdam ; New York: Elsevier. xviii, 575 p.
21. Lanao J. M., Briones E., and Colino C. I., *Recent advances in delivery systems for anti-HIV1 therapy*. J. Drug Target, 2007. **15**(1): p. 21-36.
22. Ulrich A. S., *Biophysical aspects of using liposomes as delivery vehicles.* Biosci. Rep., 2002. **22**(2): p. 129-50.
23. Hochmuth R. M., Mohandas N., and Blackshear P. L. Jr., *Measurement of the elastic modulus for red cell membrane using a fluid mechanical technique.* Biophys. J., 1973. **13**(8): p. 747-62.

24. Presley J. F., *et al*., *ER-to-Golgi transport visualized in living cells.* Nature, 1997. **389**(6646): p. 81-5.
25. Barclay T., Constantopoulos K., and Matisons J., *Self-assembled lipid nanotubes by rational design.* J.Mater.Res., 2011. **26**(2): p. 322-335.
26. Shimizu T., *Self-assembled lipid nanotube hosts: The dimension control for encapsulation of nanometer-scale guest substances.* J.Polym.Sci.Pol.Chem., 2006. **44**(17): p. 5137-5152.
27. Karlsson A., *et al., Controlled initiation of enzymatic reactions in micrometer-sized biomimetic compartments.* J. Phys. Chem. B., 2005. **109**(4): p. 1609-17.
28. Lobovkina T., *et al., Zipper dynamics of surfactant nanotube Y junctions.* Phys. Rev. Lett., 2006. **97**(18): p. 188105.
29. Sackmann E. and Tanaka M., *Supported membranes on soft polymer cushions: fabrication, characterization and applications.* Trends Biotechnol., 2000. **18**(2): p. 58-64.
30. Tokarz M., *et al*., *Single-file electrophoretic transport and counting of individual DNA molecules in surfactant nanotubes.* Proc. Natl. Acad. Sci. U. S. A., 2005. **102**(26): p. 9127-9132.
31. Torchilin V. P., *et al*., *Cell transfection in vitro and in vivo with nontoxic TAT peptide-liposome-DNA complexes.* Proc. Natl. Acad. Sci. U. S. A., 2003. **100**(4): p. 1972-7.
32. Jesorka A., Markstrom M., and Orwar O., *Controlling the internal structure of giant unilamellar vesicles by means of reversible temperature dependent sol-gel transition of internalized poly(N-isopropyl acrylamide).* Langmuir., 2005. **21**(4): p. 1230-7.
33. Roux A., *et al*., *GTP-dependent twisting of dynamin implicates constriction and tension in membrane fission.* Nature, 2006. **441**(7092): p. 528-31.
34. Roux A., *et al., A minimal system allowing tubulation with molecular motors pulling on giant liposomes.* Proc. Natl. Acad. Sci. U. S. A., 2002. **99**(8): p. 5394-9.
35. Jesorka A., *et al*., *Generation of phospholipid vesicle-nanotube networks and transport of molecules therein.* Nat. Protoc., 2011. **6**(6): p. 791-805.
36. Stepanyants N., *et al*., *Radial sizing of lipid nanotubes using membrane displacement analysis.* Nano. Lett., 2012. **12**(3): p. 1372-8.
37. Karlsson R., *et al*., *Moving-Wall-Driven Flows in Nanofluidic Systems.* Langmuir., 2002. **18**: p. 4186-4190.
38. Karlsson M., *et al., Micropipet-assisted formation of microscopic networks of unilamellar lipid bilayer nanotubes and containers.* Langmuir., 2001. **17 (22)**: p. 6754-6758.
39. Lobovkina T., *et al., Formation and release of circular lipid nanotube.* Soft Matter, 2008. **4**: p. 467-470.
40. Rustom A., *et al., Nanotubular highways for intercellular organelle transport.* Science, 2004. **303**(5660): p. 1007-10.
41. Gerdes H. H., Bukoreshtliev N. V., and Barroso J. F., *Tunneling nanotubes: a new route for the exchange of components between animal cells.* FEBS Lett., 2007. **581**(11): p. 2194-201.
42. Gerdes H. H. and Carvalho R. N., *Intercellular transfer mediated by tunneling nanotubes.* Curr. Opin. Cell. Biol., 2008. **20**(4): p. 470-5.
43. Davis D. M. and Sowinski S., *Membrane nanotubes: dynamic long-distance connections between animal cells.* Nat. Rev. Mol. Cell Biol., 2008. **9**(6): p. 431-6.
44. Gurke S., Barroso J. F., and Gerdes H. H., *The art of cellular communication: tunneling nanotubes bridge the divide.* Histochem. Cell. Biol., 2008. **129**(5): p. 539-50.
45. Veranic P., *et al., Different types of cell-to-cell connections mediated by nanotubular structures.* Biophys. J., 2008. **95**(9): p. 4416-25.

46. Wang X. and Gerdes H. H., *Long-distance electrical coupling via tunneling nanotubes.* Biochim. Biophys. Acta., 2012. **1818**(8): p. 2082-6.
47. Sowinski S., *et al.*, *Membrane nanotubes physically connect T cells over long distances presenting a novel route for HIV-1 transmission.* Nat. Cell Biol., 2008. **10**(2): p. 211-9.
48. Eugenin E. A., Gaskill P. J., and Berman J. W., *Tunneling nanotubes (TNT): A potential mechanism for intercellular HIV trafficking.* Commun. Integr. Biol., 2009. **2**(3): p. 243-4.
49. Appenzeller-Herzog C. and Hauri H. P., *The ER-Golgi intermediate compartment (ERGIC): in search of its identity and function.* J. Cell Sci., 2006. **119**(Pt 11): p. 2173-83.
50. Quehenberger O., *et al.*, *Lipidomics reveals a remarkable diversity of lipids in human plasma.* J. Lipid Res., 2010. **51**(11): p. 3299-3305.
51. Israelachvili J. N., Marcelja S., and Horn R. G., *Physical principles of membrane organization.* Q. Rev. Biophys., 1980. **13**(2): p. 121-200.
52. Jesorka A. and Orwar O., *Liposomes: Technologies and Analytical Applications*, in *Annual Review of Analytical Chemistry*. 2008, Annual Reviews: Palo Alto. p. 801-832.
53. Semple S. C., *et al.*, *Efficient encapsulation of antisense oligonucleotides in lipid vesicles using ionizable aminolipids: formation of novel small multilamellar vesicle structures.* Biochim. Biophys. Acta., 2001. **1510**(1-2): p. 152-66.
54. Okumus B., *et al.*, *Vesicle encapsulation studies reveal that single molecule ribozyme heterogeneities are intrinsic.* Biophys. J., 2004. **87**(4): p. 2798-806.
55. Banerjee R., *Liposomes: applications in medicine.* J. Biomater. Appl., 2001. **16**(1): p. 3-21.
56. Chonn A. and Cullis P. R., *Recent advances in liposomal drug-delivery systems.* Curr. Opin. Biotechnol., 1995. **6**(6): p. 698-708.
57. Mamot C., *et al.*, *Liposome-based approaches to overcome anticancer drug resistance.* Drug Resist. Updat., 2003. **6**(5): p. 271-9.
58. Reeves J.P. and Dowben R. M., *Formation and properties of thin-walled phospholipid vesicles.* J. Cell Physiol., 1969. **73**(1): p. 49-60.
59. Akashi K., *et al.*, *Preparation of giant liposomes in physiological conditions and their characterization under an optical microscope.* Biophys. J., 1996. **71**(6): p. 3242-50.
60. Criado M. and Keller B. U., *A membrane fusion strategy for single-channel recordings of membranes usually non-accessible to patch-clamp pipette electrodes.* FEBS Lett., 1987. **224**(1): p. 172-6.
61. Karlsson M., *et al.*, *Electroinjection of colloid particles and biopolymers into single unilamellar liposomes and cells for bioanalytical applications.* Anal. Chem., 2000. **72**(23): p. 5857-62.
62. Moscho A., *et al.*, *Rapid preparation of giant unilamellar vesicles.* Proc. Natl. Acad. Sci. U. S. A., 1996. **93**(21): p. 11443-7.
63. Helfrich W., *Elastic properties of lipid bilayers: theory and possible experiments.* Naturforsch. Z.C., 1973. **28**(11): p. 693-703.
64. Deuling H.J. and Helfrich W., *The curvature elasticity of fluid membranes : A catalogue of vesicle shapes.* J. Phys. France, 1976. **37**(11).
65. Rawicz W., *et al.*, *Effect of chain length and unsaturation on elasticity of lipid bilayers.* Biophys. J., 2000. **79**(1): p. 328-39.
66. Evans E. and Needham D., *Physical properties of surfactant bilayer membranes: thermal transitions, elasticity, rigidity, cohesion and colloidal interactions.* J.Phys.Chem., 1987. **91**: p. 4219-4228.

67. Olbrich K., *et al*., *Water permeability and mechanical strength of polyunsaturated lipid bilayers.* Biophys. J., 2000. **79**(1): p. 321-7.
68. Seifert U., Berndl K., and Lipowsky R., *Shape transformations of vesicles: Phase diagram for spontaneous- curvature and bilayer-coupling models.* Phys. Rev. A., 1991. **44**(2): p. 1182-1202.
69. Lipowsky R., *The conformation of membranes.* Nature, 1991. **349**(6309): p. 475-81.
70. Evans E. and Rawicz W., *Entropy-driven tension and bending elasticity in condensed-fluid membranes.* Phys. Rev. Lett., 1990. **64**(17): p. 2094-2097.
71. Zilker A., Ziegler M., and Sackmann E., *Spectral analysis of erythrocyte flickering in the 0.3-4- microm-1 regime by microinterferometry combined with fast image processing.* Phys. Rev. A, 1992. **46**(12): p. 7998-8001.
72. Seifert U. and Lipowsky R., *Adhesion of vesicles.* Phys. Rev. A., 1990. **42**(8): p. 4768-4771.
73. Blount Maurice J., Miksis Michael J., and Davis Stephen H., *The equilibria of vesicles adhered to substrates by short-ranged potentials.* P. ROY. SOC. A-MATH. PHY., 2013. **469**(2153).
74. Bernard A.-L., *et al.*, *Strong adhesion of giant vesicles on surfaces: Dynamics and permeability.* . Langmuir., 2000. **16** (17): p. 6809-6820.
75. Czolkos I., Jesorka A., and Orwar O., *Molecular phospholipid films on solid supports.* Soft Matter, 2011. **7**(10): p. 4562-4576.
76. Lou E., *et al.*, *Tunneling Nanotubes Provide a Unique Conduit for Intercellular Transfer of Cellular Contents in Human Malignant Pleural Mesothelioma.* Plos One, 2012. **7**(3).
77. Onfelt B., *et al*., *Structurally distinct membrane nanotubes between human macrophages support long-distance vesicular traffic or surfing of bacteria.* J. Immunol., 2006. **177**(12): p. 8476-83.
78. Kumar N. M. and Gilula N. B., *The gap junction communication channel.* Cell, 1996. **84**(3): p. 381-8.
79. Fevrier B. and Raposo G., *Exosomes: endosomal-derived vesicles shipping extracellular messages.* Curr. Opin. Cell Biol., 2004. **16**(4): p. 415-21.
80. Greco V., Hannus M., and Eaton S., *Argosomes: a potential vehicle for the spread of morphogens through epithelia.* Cell, 2001. **106**(5): p. 633-45.
81. Abounit S. and Zurzolo C., *Wiring through tunneling nanotubes--from electrical signals to organelle transfer.* J. Cell Sci., 2012. **125**(Pt 5): p. 1089-98.
82. Dubey G. P. and Ben-Yehuda S., *Intercellular nanotubes mediate bacterial communication.* Cell, 2011. **144**(4): p. 590-600.
83. Upadhyaya A. and Sheetz M. P., *Tension in tubulovesicular networks of Golgi and endoplasmic reticulum membranes.* Biophys. J., 2004. **86**(5): p. 2923-8.
84. Abel M. P., *et al.*, *Microstructured platforms to study nanotube-mediated long-distance cell-to-cell connections.* Biointerphases, 2011. **6**(1): p. 22-31.
85. Bozic B., *et al.*, *Role of lamellar membrane structure in tether formation from bilayer vesicles.* Biophys. J., 1992. **61**(4): p. 963-73.
86. Heinrich V. and Waugh R. E., *A piconewton force transducer and its application to measurement of the bending stiffness of phospholipid membranes.* Ann. Biomed. Eng., 1996. **24**(5): p. 595-605.
87. Cuvelier D., *et al.*, *Coalescence of membrane tethers: experiments, theory, and applications.* Biophys. J., 2005. **88**(4): p. 2714-26.
88. Evans E. and Yeung A., *Hidden dynamics in rapid changes of bilayer shape.* Chem.Phys.Lipids, 1994. **73**(1-2): p. 39-56.

89. Koster G., *et al.*, *Membrane tube formation from giant vesicles by dynamic association of motor proteins.* Proc. Natl. Acad. Sci. U. S. A., 2003. **100**(26): p. 15583-8.
90. Karlsson A., *et al.*, *Networks of nanotubes and containers.* Nature, 2001. **409**(6817): p. 150-2.
91. Karlsson M., *et al.*, *Biomimetic nanoscale reactors and networks.* Annu. Rev. Phys. Chem., 2004. **55**: p. 613-49.
92. Wilhelm C., *et al.*, *Kinetics of pore size during irreversible electrical breakdown of lipid bilayer membranes.* Biophys. J., 1993. **64**(1): p. 121-8.
93. Glaser R. W., *et al.*, *Reversible electrical breakdown of lipid bilayers: formation and evolution of pores.* Biochim. Biophys. Acta., 1988. **940**(2): p. 275-87.
94. Aimmerberg J., Cohen F.S., and Finkelstein A., *Fusion of phospholipid-vesicles with planar phospholipid-bilayer memebranes .1. Discharge of vesicular contents across the planar membrane.* J.Gen. Physiol., 1980. **75**: p. 241-250.
95. Haluska C.K., *et al.*, *Timescales of membrane fusion revealed by direct imaging of vesicle fusion with high temporal resolution.* Proc. Natl. Acad. Sci. U.S.A., 2006. **103**(43): p. 15841-15846.
96. Lobovkina T., *et al.*, *Mechanical tweezer action by self-tightening knots in surfactant nanotubes.* Proc. Natl. Acad. Sci. U. S. A., 2004. **101**(21): p. 7949-53.
97. Derenyi I., Julicher F., and Prost J., *Formation and interaction of membrane tubes.* Phys. Rev. Lett., 2002. **88**(23): p. 238101.
98. Lizana L. and Konkoli Z., *Diffusive transport in networks built of containers and tubes.* Phys. Rev. E. Stat. Nonlin. Soft Matter Phys., 2008. **72**(2 Pt 2): p. 026305.
99. Dagdug L, *et al.*, *Equilibration in two chambers connected by a capillary.* Phys. Rev. E, 2003. **119** (23): p. 12473-12478.
100. Stange P., *et al.*, *Self-organizing molecular networks.* Biophys. Chem., 1998. **72**(1-2): p. 73-85.
101. Pedro P., *et al.*, *Membrane nanotubes drawn by optical tweezers transmit electrical signals between mammalian cells over long distances.* Lab on a Chip, 2010. **10**(17): p. 2235-2241.
102. Hubbell W. L. and Mcconnel Hm., *Molecular Motion in Spin-Labeled Phospholipids and Membranes.* J. Am. Chem. Soc., 1970. **93**(2): p. 314-&.
103. Czolkos I., *et al.*, *High-resolution micropatterned Teflon AF substrates for biocompatible nanofluidic devices.* Langmuir., 2012. **28**(6): p. 3200-5.
104. Voldman J., Gray M. L., and Schmidt M.A., *Microfabrication in Biology and Medicine.* Annu. Rev. Biomed. Eng., 1999. **1**(1): p. 401-425.
105. Zhang D. Y., Men L. Q., and Chen Q. Y., *Microfabrication and Applications of Opto-Microfluidic Sensors.* Sensors, 2011. **11**(5): p. 5360-5382.
106. Hochrein M. B., *et al.*, *DNA molecules on periodically microstructured lipid membranes: localization and coil stretching.* Phys. Rev. E. Stat. Nonlin. Soft. Matter. Phys., 2007. **75**(2 Pt 1): p. 021901.
107. Weibel D. B., Diluzio W. R., and Whitesides G. M., *Microfabrication meets microbiology.* Nat. Rev. Microbiol., 2007. **5**(3): p. 209-18.
108. Ainla A., *et al.*, *A microfluidic diluter based on pulse width flow modulation.* Anal. Chem., 2009. **81**(13): p. 5549-56.
109. Connelly J. T., *et al.*, *Micro-total analysis system for virus detection: microfluidic pre-concentration coupled to liposome-based detection.* Anal. Bioanal. Chem., 2012. **402**(1): p. 315-23.
110. Mark D., *et al.*, *Microfluidic lab-on-a-chip platforms: requirements, characteristics and applications.* Chem. Soc. Rev., 2010. **39**(3): p. 1153-82.

111. Tegenfeldt J. O., *et al*., *From the Cover: The dynamics of genomic-length DNA molecules in 100-nm channels.* Proc. Natl. Acad. Sci. U. S. A., 2004. **101**(30): p. 10979-83.
112. Levy S. L. and Craighead H. G., *DNA manipulation, sorting, and mapping in nanofluidic systems.* Chem. Soc. Rev., 2010. **39**(3): p. 1133-52.
113. Leggett G. J., *Scanning near-field photolithography--surface photochemistry with nanoscale spatial resolution.* Chem. Soc. Rev., 2006. **35**(11): p. 1150-61.
114. Yang C. B., *Nanoscale line segment fabrication using super-resolution near-field photolithography.* Scanning, 2012. **34**(5): p. 284-94.
115. Yang C. B., Chiang H.L., and Huang J.C., *Study on advanced nanoscale near-field photolithography.* Scanning, 2010. **32**(6): p. 351-60.
116. Nishikubo T. and Kudo H., *Recent development in molecular resists for extreme ultraviolet lithography.* J. Photopolym. Sci. Tec., 2011. **24**: p. 9-18.
117. Pinnau I. and Toy L.G., *Gas and vapor transport properties of amorphous perfluorinated copolymer membranes based on 2,2-bistrifluoromethyl-4,5-difluoro-1,3-dioxole/tetrafluoroethylene.* J. Membrane Sci., 1996. **109**(1): p. 125-133.
118. Makohliso S. A., *et al., Application of Teflon-AF thin films for bio-patterning of neural cell adhesion.* Biosens Bioelectron, 1998. **13**(11): p. 1227-35.
119. Thomas C. H., *et al., Surfaces designed to control the projected area and shape of individual cells.* J. Biomech. Eng., 1999. **121**(1): p. 40-8.
120. Datta A., *et al., Microfabrication and Characterization of Teflon AF-Coated Liquid Core Waveguide Channels in Silicon.* IEEE. Sens.J., 2003. **3** (6): p. 788-795.
121. Mertz J., *Introduction to optical microscopy*. 2010, Greenwood Village, Colo.: Roberts. xviii, 413 p.
122. Dommersnes P. G., *et al., Marangoni transport in lipid nanotubes.* EPL (Europhysics Letters), 2005. **70**: p. 271.